TRIBHUVAN UNIVERSITY

INSTITUTE OF ENGINEERING

PULCHOWK CAMPUS

Thesis no: M-65-MSMDE-2017-2023

Experimental Evaluation of Payload Induced Oscillations of an Unmanned Rotorcraft System

By

Bimal Bhattarai

A FINAL THESIS REPORT
SUBMITTED TO THE DEPARTMENT OF MECHANICAL AND AEROSPACE ENGINEERING IN PARTIAL FULFILLMENT OF THE REQUIREMENTS FOR THE DEGREE OF MASTERS OF SCIENCE IN
MECHANICAL SYSTEMS DESIGN AND ENGINEERING

DEPARTMENT OF MECHANICAL AND AEROSPACE ENGINEERING

LALITPUR, NEPAL

AUGUST, 2023

COPYRIGHT

TRIBHUVAN UNIVERSITY

INSTITUTE OF ENGINEERING

PULCHOWK CAMPUS

DEPARTMENT OF MECHANICAL AND AEROSPACE ENGINEERING

The undersigned certify that they have read, and recommended to the Institute of Engineering for acceptance, a thesis entitled "Experimental Evaluation of Payload Induced Oscillation in an Unmanned Rotorcraft System" submitted by Bimal Bhattarai, in partial fulfillment of the requirements for the degree of Master of Science in Mechanical System Design and Engineering.

Supervisor, Prof. Laxman Poudel, PhD	Co-supervisor, Asst. Prof. Sudip Bhattrai, PhD
Department of Mechanical and Aerospace Engineering	Department of Mechanical and Aerospace Engineering
External Examiner, Er. Madan Timsina	Committee Chairperson
Deputy Managing Director,	Head of Department
Nepal Electricity Authority	Department of Mechanical and Aerospace Engineering

Date: August 8, 2023

ABSTRACT

Among the wide-ranging fields of application for Unmanned Aerial Vehicles (UAV), Aerial delivery has demonstrated a high potential to become a mainstream delivery service in e-commerce industries. Compared to other methods of payload carriage with a UAV, a tethered carriage can be a flexible and heavy load capacity system. However, the change in dynamics of a rotorcraft due to a tethered payload leads to instability and reduced efficiency on a mission of the Unmanned Rotorcraft System (URS). This study analyzes the performance of a quadrotor during different segments of its flight, including takeoff, cruising, and landing to gain a more detailed understanding of its behavior and capabilities. For this study, Pixhawk 4 controller-based quadrotor was assembled on an S500 frame due to its ubiquitous use in academia. The payload-induced oscillation data in non-dimensionalized tether length and payload weight were studied by flying the URS in two distinct autonomous missions. The autonomous mission was set and controlled using qgroundcontrol, an open-source ground station system for Pixhawk controller. Furthermore, the inevitable vibrations due to extraneous factors were evaluated by conducting the autonomous mission with and without load conditions separately. Thus, obtained data were assessed case-specifically for different values of cable length, payload mass, speed, and altitude. In order to harmonize the time duration of the total flight and flight time of each segment, the time factor was normalized to define all possible cases. These data were analyzed and plotted in MATLAB to study the effect of change in variables on the preset autonomous missions. This study found that destabilizing effect of an underactuated cable-suspended payload caused secondary oscillations. Also, with increasing cable length and increasing payload mass, the pitch, roll, and altitude fluctuations were found to increase significantly in all cases with the tethered payload attached to the URS. However, the time period of pitch angle oscillation decreases by 28.3% when speed is increased from 5m/s to 7m/s on a segment of quadrilateral path. Each segment of the flight path is studied in details. So, in order to address the fluctuation and deviation characteristics of the quadrotor, further consideration in the control scheme for the quadrotor control system.

ACKNOWLEDGMENT

I would like to offer my deepest gratitude to Dr. Laxman Poudel, who has been my academic supervisor and provided invaluable support and guidance throughout this research work. His contributions have significantly improved the quality of this thesis. Additionally, I extend my sincere thanks to Dr. Sudip Bhattrai for serving as my co-supervisor and providing continuous feedback, comments, and valuable advice during the course of this research. His expertise and mentorship have been instrumental in shaping the direction of this study.

Further, I thank Dr. Hari Bahadur Darlami and Dr. Nawaraj Bhattarai for their insightful feedback during the presentation phase, which helped me refine my research and present it more effectively. Also, I would also like to acknowledge the moral support and useful instructions I received from Dr. Ajay Kumar Jha, which played a crucial role in motivating and guiding me during the problem identification and research phase.

Moreover, I am especially thankful to Er. Biman Rimal, Mr. Apil Ghimire, and Er. Ashish Karki for providing valuable support and guidance during my study's experimentation, and data collection stage. On top of this, I extend my hearty appreciation to my friend Er. Asbina Baral for her support and valuable insights during every stage of this research.

Additionally, I would like to express my sincere thanks to the Nepal Academy of Science and Technology (NAST) for providing a Master's thesis grant that greatly supported this research work. The financial assistance offered by NAST was very helpful in purchasing tools, equipment, and materials required for the experimentation phase of this thesis.

Lastly, I am deeply indebted to my family, friends, and seniors for being a great source of inspiration, encouragement, and guidance throughout my study.

To all those mentioned above, as well as to those not explicitly named but who have contributed in their own ways, I offer my sincerest thanks for making this thesis possible. Your support has been invaluable and deeply appreciated.

TABLE OF CONTENTS

LIST OF TABLES

LIST OF FIGURES

LIST OF SYMBOLS

θ	Pitch Angle
ψ	Yaw Angle
ϕ	Roll Angle
Ψ	Attitude vector. $\Psi = [\phi\ \theta\ \psi]$
M	Non-Dimensional Mass
L	Non-Dimensional Length
M_p	Mass of Payload
M_Q	Mass of Quadrotor
L_c	Length of suspension cable from CoG
L_{qa}	Length of quadrotor arm
M_n	Non-Dimensional Mass for ‘n’ payload Mass
L_n	Non-Dimensional Length for ‘n’ cable length
x	Translation along x axis
y	Translation along y axis
z	Translation along z axis
T	Total time for autonomous mission
r	Position vector r = [x y z]
v	Velocity vector
l	Moments around coordinate axis x
m	Moments around coordinate axis y
n	Moments around coordinate axis z.
M	Moment vector M = [l m n]
F	Force, Thrust
q	Quaternion

LIST OF ABBREVIATIONS

URS	Unmanned Rotorcraft Systems
UAS	Unmanned Aerial Systems
UAV	Unmanned Aerial Vehicles
RC	Remote Controlled
ESC	Electronic Speed Controller
CoG	Centre of Gravity
NDM	Non-Dimensionalized mass
NDL	Non-Dimensionalized Length
IMU	Inertial Measurement Unit
GPS	Global Positioning system
FFT	Fast Fourier Transform
BLDC	Brushless Direct Current
PSD	Power Spectrum Density
MATLAB	Matrix Laboratory
P	Proportional
PD	Proportional-Derivative
PID	Proportional-Inegral-Derivative
EKF	Extended Kalman Filter (First Generation)
EKF2	Extended Kalman Filter (Second Generation)
MEMS	Micro electro-mechanical systems
GNSS	Global Navigation Satellite System

CHAPTER ONE: INTRODUCTION

1.1 Background

Even today, there are many places in Nepal that are disconnected from road network, that rely on delivery goods and supplies from air. Delivery of goods and supplies with drone is seen as very viable solution to this grave problem. Of the many delivery options, delivery with suspended cable is very viable solution as it does not require landing of vehicle for the delivery. Although different system with suspended cable is being used in Nepal, for example in setting up transmission line, delivery of bulk cargo for projects in remote areas, scaling these feats to a highly mobile autonomous quadrotors or other forms of Unmanned Aerial Systems (UAS) will open up a large application in our country.

A quadrotor is one of the different types of Unmanned Aerial Vehicles (UAVs) that can carry a payload as a form of aerial logistics transport. They are versatile and powerful tools with a wide range of uses, including disaster relief, agriculture, wildlife monitoring, and more. They can transport payloads to inaccessible locations, making them invaluable in various industries and humanitarian efforts. Advances in quadrotor technology are continually expanding their capabilities and potential impact across many fields.

A Quadrotor system can operate autonomously with the onboard controller or remote-controlled (RC) piloting. A quadrotor UAV system generally consists of different onboard sensors, payloads, and rotorcraft components, such as frames, motors, Electronic Speed Controller (ESC) and a ground control station.

Transport of different payloads using multi-rotor systems has shown a promising application in many areas in recent years. The challenging nature of civilian and military applications has attracted much attention to developing a reliable payload system. In situations where, traditional ground vehicles are unable to be used, aerial vehicles becomes the only option to address the transportation needs. For instance, they are necessary when providing relief materials and first aid during rescue missions in flood situations, providing basic survival kits to stranded persons on adventure sports. Rotorcraft, such as helicopters and quadrotors, are specialized to applications that require hovering and vertical take-off. Compared to helicopters, quadrotors have many

advantages because they have four rotors that facilitate load distribution and are smaller in size. Additionally, smaller rotors limit the degree of damage in the case of a crash.(Omar, Akram, et al., 2022). Also, other vehicle protection, such as a rotor guard around the rotor, can reduce the severity and damage to the whole of the aircraft.

In this modern age, the aerial delivery of packages has important potential for application for multi-rotor vehicles. Many large multi-national companies, such as Amazon, have started offering this service, and many are researching to improve payload delivery methods (Sunghun & su, 2017). Moreover, leading global service companies announced that they are supporting research and development projects on the use of UAVs for package delivery (Us et al., 2019). There are two options for attaching cargo to a quadrotor: a rigid connection or a suspension beneath the vehicle by a cable. While the rigid connection is commonly used because of its practicality and simplicity, it may not be suitable for heavy or oversized packages and may not always allow for landing in desired locations. Additionally, this configuration can cause significant increase the quadrotor's inertia and decrease its maneuverability. On the other hand, oversized packages are able to be carried with one or more quadrotors working in a coordinated flight with a suspended load (Omar, Fortuna, et al., 2022). With this setup, the package can be delivered without the need for the vehicle to land, which makes the mission more efficient. However, this method can make it more difficult to control the quadrotor, especially when it comes to managing the position of the payload in windy conditions. As a result, researchers have been working on developing control systems for quadrotors that carry suspended loads. This is to help stabilize the vehicle and prevent any oscillations in the load, while ensuring accurate pickup and positioning of the payload.

1.2 Problem Statement

In recent years, the utilization of Unmanned Rotorcraft Systems (URS) like quadrotor drones for the delivery of goods has become increasingly popular. Major e-commerce companies have invested in research to improve this technology. However, one major challenge that URS technology faces is the oscillations induced in the system during operation, which can lead to unreliable payload delivery. To minimize these oscillations, path optimization and active control systems are required.

The development of a control system to attenuate oscillations in any scale requires non-dimensionalized oscillation and vibration data. Such data can help identify the effect of various flight parameters on the vehicle and in turn, aid in the design of optimized flight trajectories and active actuator control for URS of any scale.

Based on my research, there is currently no available work on vibration and flight path data for the Pixhawk controller, which is an open-source platform for a cable-suspended payload. Therefore, the purpose of this paper is to evaluate and illustrate the characteristics of a quadrotor-based on the Pixhawk controller, with a cable-suspended load. This evaluation aims to aid in the development of a control system that can minimize payload oscillations.

By establishing a non-dimensionalized data set for a quadrotor system with a cable-suspended payload, even larger delivery systems can be designed. This technology would be particularly useful for post-disaster relief management and general delivery systems. The data obtained from this study can serve as a basis for future research to further improve the delivery capabilities of URS which will be useful in post-disaster relief management, and general delivery system.

1.3 Objectives

1.3.1 Main Objective

The main objective of this study is to experimentally evaluate the oscillations data for the Unmanned Rotorcraft System (URS) with tethered payload.

1.3.2 Specific Objectives

The main objectives will be accomplished with the following auxiliary objectives:

1. To study the characteristics of URS with tethered payload on take-off, cruise, and landing Segments of the mission.
2. To study the effect of payload mass and cable length on URS performance.
3. To study the effect of speed on URS performance.

1.4 Scope of Work

This study is mainly focused on determining the flight and vehicle oscillation characteristics of Pixhawk based quadrotor under cable suspended load system. With this data from experimentation, different visualization of various cases of the flight and corresponding flight path of the vehicle will be represented in this study. And, a set of vehicular characteristics data will be developed for further development in suspended payload oscillation and dynamic characteristics as desired with the implementation of advanced algorithms, such as reinforcement learning, and predictive model-based control approaches. Due to non-dimensional quantity, this study can be used to validate scaled model of similar mission profile with path variables.

CHAPTER TWO: LITERATURE REVIEW

2.1 Quadrotor System

A quadrotor, which is an unmanned aerial vehicle (UAV), is equipped with four rotors that are strategically arranged in a cross configuration to maintain stability. These rotors can operate independently to control thrust and torque, allowing the quadrotor to move in six different directions: up and down, forward and backward, left and right, and around the x, y, and z axes. However, due to its design, the quadrotor is classified as underactuated, meaning it has more degrees of freedom than control inputs. Consequently, it can be challenging to accurately control its position and orientation, particularly during takeoff and landing when faced with wind gusts. Therefore, developing stabilization methods is crucial to counteract these instabilities and address the underactuated nature of the quadrotor system.

As discussed already, it is a challenging task to maintain stability and smooth operation in a quadrotor due to its inherent nature. Adding to this, if a payload is suspended with a tether it brings on even more external instabilities and disturbances that the quadrotor has to deal with. These instabilities and disturbances are mainly caused by the added inertia due to payload on the quadrotor's dynamics, and increased power requirement on the motors and propellers.

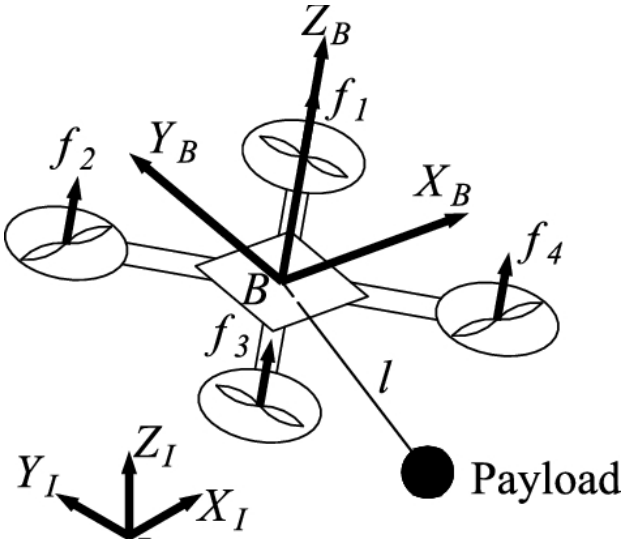

Figure 2.1: Quadrotor System with Suspended payload (Alkomy & Shan, 2021)

2.1.1 Axis of Movement for the Quadrotor

A rigid body remains fixed in its orientation and position in space, regardless of the coordinate system being used. To describe the orientation of an object, Tait-Bryan Angles are utilized. These angles are a variation of the Proper Euler Angles and represent the object's rotation around three different axes, known as roll, pitch, and yaw angles. These angles are commonly used in aviation to describe an aircraft's orientation (Bhattarai et al., 2018). Pitch, yaw, and roll are the three basic movements of a quadcopter. They are used to control the quadcopter's position and orientation in space.

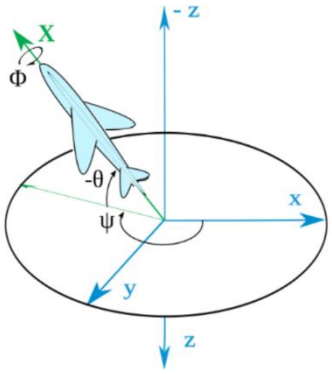

Figure 2.2: Tait-Bryan angles for orientation of objects in space (Bhattarai et al., 2018)

Pitch and Pitch angle (θ): Pitch is the movement of the quadcopter's nose up or down. It is controlled by increasing or decreasing the speed of the rotors on the front and back of the quadcopter. If the front rotors are sped up, the nose of the quadcopter will pitch up. If the back rotors are sped up, the nose of the quadcopter will pitch down. The pitch is the most important movement for controlling the quadcopter's altitude. By pitching up or down, the quadcopter can ascend or descend. Pitch angle is denoted with θ.

Yaw and Yaw angle (ψ): Yaw is the movement of the quadcopter's nose left or right. It is controlled by increasing or decreasing the speed of the rotors on the left and right of the quadcopter. If the left rotors are sped up, the nose of the quadcopter will yaw to the left. If the right rotors are sped up, the nose of the quadcopter will yaw to the right. Yaw is used to control the quadcopter's direction of travel. By yawing left or right, the quadcopter can move in any direction. Yaw angle is denoted with the symbol ψ.

Roll and Roll angle (ϕ): *Roll* is the movement of the quadcopter's body left or right. It is controlled by increasing or decreasing the speed of the rotors on the diagonals of the quadcopter. If the front-left rotor is sped up, the quadcopter will roll to the left. If the

back-right rotor is sped up, the quadcopter will roll to the right. Roll is used to make the quadcopter turn. By rolling left or right, the quadcopter can make a turn. Roll angle is denoted with the symbol ϕ.

By combining these three movements, a quadcopter can be controlled to move in any direction in space.

2.1.2 Cable Suspended Payload Quadrotor System

A quadrotor consists of a frame and motors that generate the necessary forces to lift and propel the vehicle. The suspended load is connected to the center of the quadrotor's frame., as illustrated in Figure 2.2.

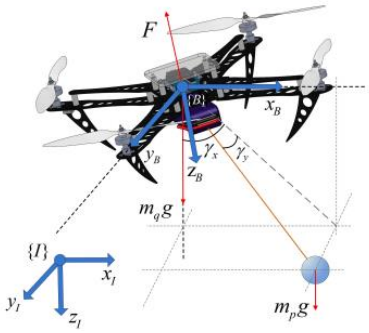

Figure 2.3: Quadrotor multi-body system with cable suspended payload (Xian et al., 2020)

A quadrotor with a tethered payload system exhibits a multi-body dynamics due to the interaction of the vehicle and payload dynamics. As a typical under-actuated mechanical system, the quadrotor has only four inputs for inputs, but six outputs on motion (Emran & Najjaran, 2018). The under-actuated nature of a quadrotor with a tethered payload is more complicated than an underactuated system, since there is no control input in order to constrain the payload movement (Xian et al., 2020). This requires means to attenuate the undesired movement of the payload and the corresponding effect on the quadrotor system.

2.2 Study of Past Research

Many academics have studied different cable-suspended payload systems recently and suggested about its special dynamics, and also some of them suggesting method of control for controlling the payload and UAV dynamics. On a UAV the purpose of a controller is to stabilize the UAV during take-off, hovering state, on cruise along a

defined trajectory, and landing stages; with the extension of the controller scope to the payload as well, the controller frequently adjust the payload swing by managing its dynamics to reduce the payload's swinging motion. (Roy et al., 2021)

Various control algorithms have been suggested in literature for quadcopters without a suspended load. These controllers include Proportional Integral Derivative (PID) controller(Pounds et al., 2012), Linear Quadratic Regulator/Gaussian-LQR/G (Han et al., 2018), Sliding Mode Control (SMC) (Zhou et al., 2016) , Optimal Control Algorithms, Feedback Linearization, Intelligent Control (Fuzzy Logic and Artificial Neural Networks), Adaptive Control Algorithms, Integrator Back-stepping Control, Robust Control Algorithms, and Hybrid Control Algorithms (Omar, Fortuna, et al., 2022). However, when a suspended payload is added, it is crucial to control and dampen the oscillation of the payload within certain limitations.

Zhou et al., (2016) suggested an adaptive controller to address the issue of a suspended load, but it was based on the assumption that the load was connected directly to the quadrotor. This assumption results in a less complex dynamic model, which means the method may not be suitable for a suspended load scenario. To maintain balance and perform various tasks, other control algorithms have been tested and implemented on a quadrotor system with a suspended payload. These algorithms include classic PD control. (Estevez et al., 2021), back-stepping control (Zhou et al., 2016), fuzzy and neural network control, linear and nonlinear state feedback control, Nonlinear Model Predictive Control (NMPC) (Guo et al., 2013), PID control (Pounds et al., 2012), sliding mode control, and passivity-based control (Meissen et al., 2017).

The available literatures on cable-suspended payload systems covers various stages of flight and mission segments of the system, with specific attention given to the configuration of payloads connected to UAVs for the purpose of delivering packages for different application scanarios. To move from theory to practical applications, it is necessary to examine the "mission segments" of the flight. An autonomous quadrotor mission can be broken down into three primary segments that need to be studied.

1) Take-off to First hover condition,

2) Normal cruise fight along defined trajectory, and

3) Landing and touchdown

2.2.1 Takeoff to first hover condition

The first segment of the UAV mission is the launch or take-off segment. This stage involves initializing the UAV and smoothly raising the payload from the ground using a suspension cable. Alothman et al., (2015) evaluated the performance of both an PD controller and a LQR controller during this specific phase. Through simulations, they found the LQR controller to be more effective. Faust et al., (2017) also studied the takeoff process for a UAV-slung payload. They emphasized the importance of completing this step smoothly before proceeding with the transportation of cargo. The researchers presented a method that involves three modes: UAV setup, initial pull, and raise to the initial waypoint. During the setup phase the UAV to take off the ground and then moves to a position that is directly above the payload while maintaining the cable without any tension along it. After the setup phase the initial pull phase begins, during this phase vehicle gains altitude to a state that the tether just develops tension due to the payload pull. Finally, during the raise to the initial waypoint stage UAV lifts the payload off the ground into the air, thus completing the takeoff to first hover condition. All in all, this hybrid approach was found to be successful to lift the payload smoothly from the ground, which is very crucial the initial step during any type of payload transportation mission profile (Kevin & Graham, 2019).

2.2.2 Normal Cruise Flight

Regarding the primary aspect of transportation missions, specifically the flight between two points, significant progress has been made on the subject. Researchers who study the system of payloads carried by UAVs have mainly focused on creating controllers that can fly along a predetermined path. Palunko et al., (2012) have emphasized on importance of generation of a trajectory for the UAV to reduces the tethered payload swing and consequent UAV disturbances when cruising along a predetermined path on a mission profile. The planning, generation and execution of path tracking of the UAV along the cruise trajectory of the mission profile is considered to be the most crucial to maintain the payload swing to an acceptable limit and also to maintain the integrity of payload, therefore, a lot of effort has been invested in addressing this issue.

In their study, Yi et al., (2017) introduced a sliding mode controller for quadrotors that could follow a predetermined path without requiring explicit payload feedback.

Although the simulation results were promising, the flight scenario revealed that disturbances such as wind or swinging payload could pose a significant challenge during cruising.

To address this issue, Nicotra et al., (2014) developed and presented a controller with some level of robustness against payload's fluctuations and disturbances. Qian & Liu, (2017) developed a trajectory cruising controller designed explicitly for tethered payload systems to withstand wind disturbances. Moreover, Guerrero-Sánchez et al. (2017) proposed a passivity based system that could attenuate the swinging motion and attitude fluctuations of a tethered payload during a trajectory or cruise mission profile. Meissen et al., (2017) conducted a study of for payload induced oscillations, and found that the swing motion was effectively suppressed along the flight trajectory and the oscillations were independent of the sway angle of the tethered payload.

Previous methods for controlling the oscillations and resulting fluctuations of a tethered payload on a UAV are based on traditional control theory approach. However, recent studies have delved into the use of advanced method of control such as Reinforcement Learning (RL) in order to address mission tracking challenges associated with cable suspended payload system. In their research, Faust et al., (2017) utilized advanced data based reinforcement learning to execute mission path tracking and its control while trying to learn and optimize the trajectories swing-free path for tethered payload. This innovative approach has proven effective, as the RL based advanced controllers exhibit less payload oscillations and fluctuations during responsive, dynamic complex maneuvers while following along a specific trajectory. However, it is important to note that this method requires flights on numerous mission and segments to learn and reinforce better control strategy. To mitigate this challenge, simulations can be utilized to learn flight schemes over many repetitions, though it is crucial to ensure that the dynamics of the simulation platform to match with the experimental UAV setup for a seamless transition to experimental test flight from the developed simulation model.

These developments in controller design demonstrate the ongoing efforts to overcome challenges faced by quadrotors during flight. By implementing these innovative solutions, quadrotors can better navigate through various environmental factors and effectively complete their missions.

2.2.3 Landing and Touchdown

Numerous research studies have been carried out to analyze quadrotor landing missions. One particular method that has piqued interest involves the delivery stage of the suspended load. Goodarzi, (2016) conducted a study on this method, which involved the use of a cable that could be adjusted in length to gradually lower the payload to the desired delivery point while the quadrotor remained airborne. Although the author demonstrated this approach in simulation, Lee et al., (2019) have conducted further research to explore experimental applications that involve an additional payload-lowering mechanism.

2.3 PX4 Autopilot System and Pixhawk4® Controller

An autopilot system is a set of electronic devices that autonomously controls the flight of an aircraft. In the case of a quadrotor, an autopilot system uses sensors such as GPS, IMU, and cameras to determine the vehicle's position, orientation, and velocity. It then uses this information to calculate the control inputs that are necessary to keep the vehicle flying in the desired path. In an autonomous mission, the autopilot system is responsible for carrying out all flight control tasks without human input. This includes taking off, landing, and navigating to a target. There are many commercial-grade autopilots available in the market. However, Pixhawk with PX4 firmware is an open-source autopilot with wide-ranging community support. (*PX4 User Guide*, n.d.)

Due to Pixhawks's open-source nature, it is widely popular among academicians and the quadrotor community worldwide. This foster support on wide-ranging issues already solved and tested by other users worldwide. It is optimized to run PX4 v1.7 and later and is suitable for academic and commercial developers. It is based on the Pixhawk-project FMUv5 open hardware design and runs PX4 on the NuttX OS. (*PX4 User Guide*, n.d.)

The Pixhawk system consists of several components, including a flight management unit (FMU), which is responsible for controlling the drone’s movements, and a variety of sensors, actuators, and other peripherals that provide additional functionality. The system also includes a ground control station (GCS) that allows users to communicate with the drone and control its movements.(*PX4 User Guide*, n.d.)

One of the key features of the Pixhawk system is its use of the MAVLink protocol, which is a lightweight messaging protocol for communicating with drones and other unmanned systems. MAVLink allows the GCS to send commands to the drone and receive telemetry data from it in real-time.(*PX4 User Guide*, n.d.)

The following picture shows a flowchart diagram of the software and hardware components of a drone using the Pixhawk autopilot system. The diagram is divided into two main sections: the ground control and the flight controller. this diagram provides an overview of the different components that make up a drone using the Pixhawk autopilot system and how they work together to control the drone's movements and collect data.

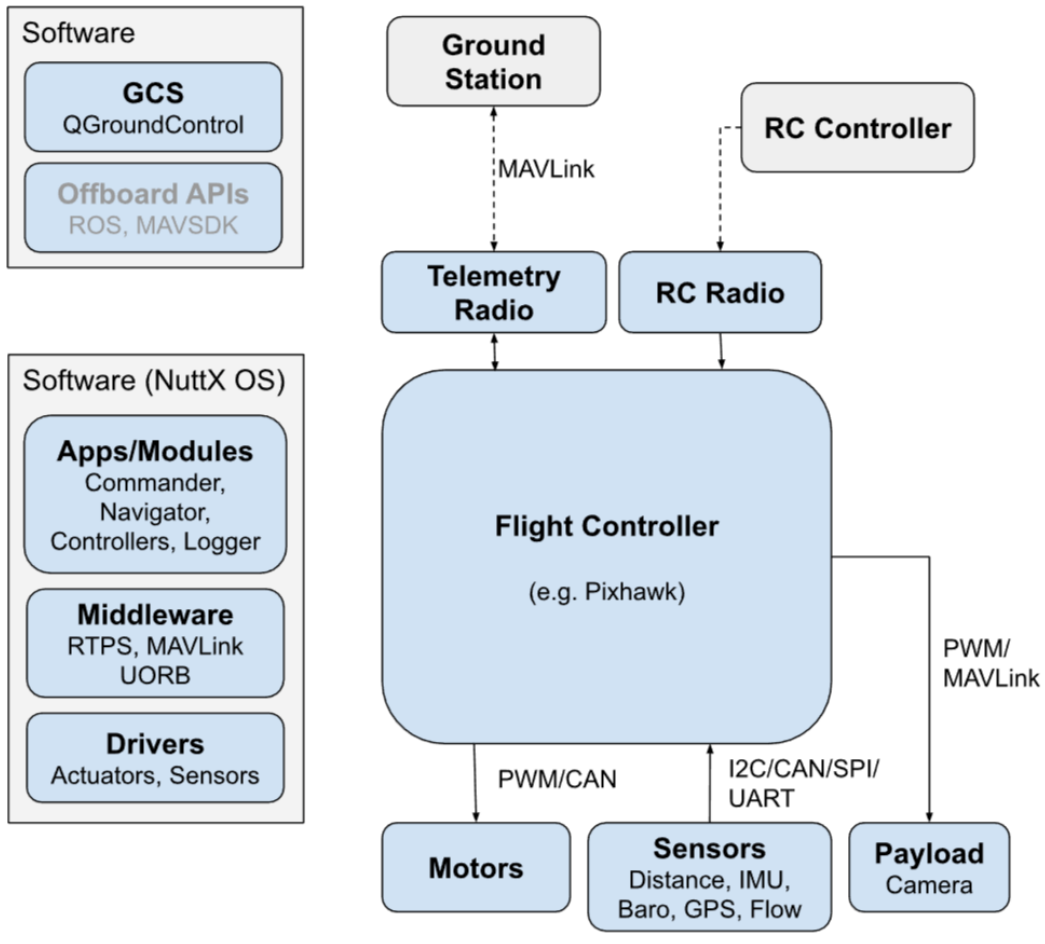

Figure 2.4 General schematic for a PX4 autopilot system (Source:(PX4 User Guide, n.d.))

The ground control section consists of several components, including Offboard APIs, MAVLink, RC Controller, Telemetry Radio, and RC Radio. These components are responsible for communicating with the drone and controlling its movements.

The flight controller section consists of several components as well, including software (NuttX OS), apps/modules (Commander, Navigator, Middleware, Logger), drivers (Actuators, Sensors, ORB), motors, sensors (Distance, IMU, Baro, GPS, Flow), and a payload camera. These components are responsible for controlling the drone's movements and collecting data.

The two sections are connected by several interfaces, including PWM, MAVLink, RTPS, I2C/CAN/SPI, UART, and USB. These interfaces allow the ground control and flight controller to communicate with each other and exchange data.(*PX4 User Guide*, n.d.)

Pixhawk controller houses the following sensors:

- *Accelerometer:* Measures the acceleration of the aircraft in three axes. These are sensitive to the vibration of the vehicle. Therefore, these sensors can provide the levels of vibration in vehicles in relation to three axes of movement.
- *Gyroscope:* Measures the rotation of the aircraft in three axes.
- *Magnetometer:* Measures the magnetic field strength in three axes.
- *Barometer:* Measures the atmospheric pressure.
- *GPS receiver:* Provides the aircraft's position and altitude.

With these in-built sensors, a continuous stream of data can be logged and later reviewed in order to determine the vehicle state and performance during the whole autonomous mission of a UAV. In addition, Pixhawk supports a wide range of peripherals, such as GPS modules, sensors, cameras, and communication protocols. This versatility enables seamless integration of additional functionalities into the system, making it suitable for a diverse set of missions.

2.3.1 Pixhawk4® Control System

General Multicopter control architecture of Pixhawk controller is as shown in the schematic below.

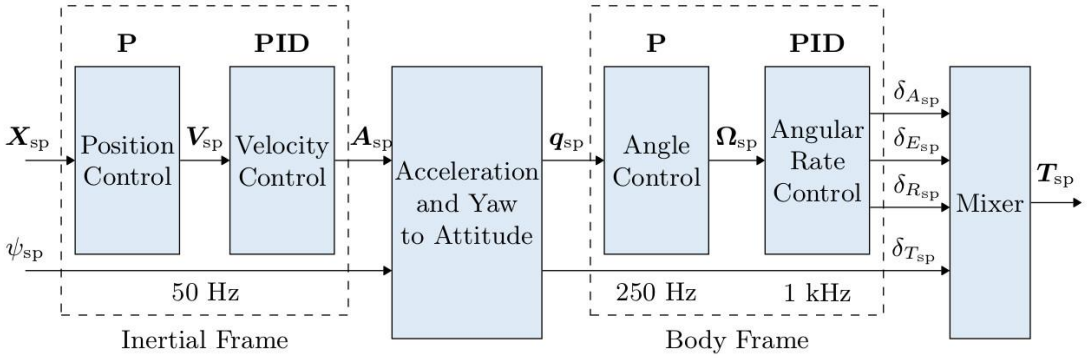

Figure 2.5 Control architecture of Pixhawk4® Multicopter controller (Source: (*PX4 User Guide*, n.d.))

- This is a standard cascaded control architecture that is implemented on the Pixhawk 4 controller.
- The controllers are a mix of P and PID controllers.
- All positions and attitude estimates come from EKF2 that is second generation of Extended Kalman Filter.
- Depending on the mode, the outer (position) loop is bypassed (shown as a multiplexer after the outer loop). The position loop is only used when holding position or when the requested velocity in an axis is null.

Multicopter Attitude Controller

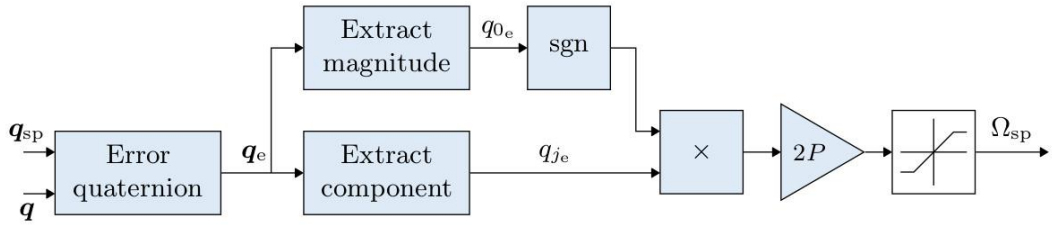

Figure 2.6 Pixhawk4® multicopter attitude controller (Source: (*PX4 User Guide*, n.d.))

- Quaternions are used for the attitude control in this controller.
- A quaternion is a complex number of the form w + xi + yj + zk, where w, x, y, and z are real numbers and i, j, and k are imaginary units that satisfy certain conditions
- When tuning this controller, the only parameter of concern is the P gain.

Multicopter Position Controller

The Pixhawk uses estimated state feedback to control the position of the quadrotor. This is accomplished by inputting the estimated position into the controller, which then calculates the desired attitude and thrust commands to control the quadrotor's motion. The estimated position is determined through a combination of the Pixhawk's onboard sensors and external sensors such as GPS or vision-based systems. The control system

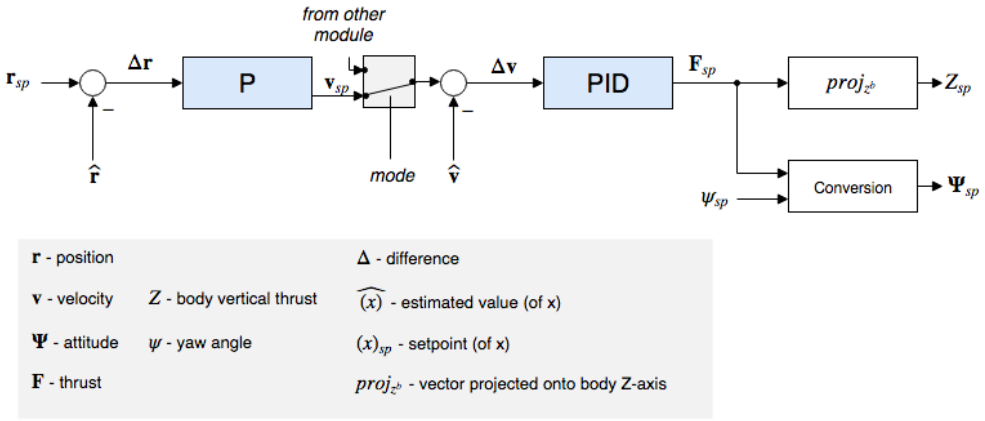

Figure 2.7 Pixhawk4® position controller (Source: (*PX4 User Guide*, n.d.))

utilizes a PID controller to generate the control commands, which are then sent to the quadrotor's motors in order to adjust its attitude and thrust.(Brescianini et al., 2013)

2.3.2 Sensors on Pixhawk4® Autopilot

In order to achieve stability and autonomous control, PX4-based systems utilize sensors to determine the vehicle's state. This includes factors such as position, altitude, heading, speed, airspeed, orientation, and rates of rotation. A gyroscope, accelerometer, magnetometer, and barometer are the minimum required sensors for the system to function. To enable automatic modes and certain assisted modes, a GPS or other positioning system is necessary. The Pixhawk Series flight controllers already incorporate the necessary minimum sensors, but additional or external sensors can be attached to the controller if needed.

2.3.2.1 Accelerometer and Gyroscope sensors

The Pixhawk 4 uses the Accel/Gyro devices to measure the attitude and movement of the drone, and to provide feedback to the flight controller for stabilization and navigation. The choice of Accel/Gyro device depends on the performance requirements and preferences of the user. For example, the BMI055 has a closed-loop gyroscope that has better bias stability and temperature compensation than the open-loop gyroscopes

of the ICM-20689 and ICM206025. However, the ICM-20689 and ICM20602 have lower noise density and power consumption than the BMI0551 (Farnell. (n.d.); TDK InvenSense. (n.d.)).

The ICM-20689 is a 6-axis Inertial Measurement Unit (IMU) manufactured by InvenSense (now part of TDK). It integrates a 3-axis accelerometer and a 3-axis gyroscope with high precision and low noise characteristics. The accelerometer is based on Microelectromechanical Systems (MEMS) technology and measures linear acceleration along the X, Y, and Z axes. The gyroscope also uses MEMS technology to sense angular velocity around these three axes. The ICM-20689 employs advanced sensor fusion algorithms, such as Kalman filtering, to combine the data from both sensors, producing accurate and reliable motion tracking information. It also supports a number of features that are not available on the other sensors, such as quaternion output and 9-axis sensor fusion, I2C and SPI communication protocols (TDK InvenSense. (n.d.)).

Similarly, the BMI055 is another 6-axis IMU designed by Bosch Sensortec. It features a triaxial accelerometer and gyroscope, utilizing MEMS technology for each sensor element. The BMI055 provides precise measurements of linear acceleration and angular velocity along the three spatial axes. It is known for its low power consumption and high stability, making it suitable for battery-powered applications like drones and other robotic systems (TDK. (2018)).

The ICM20602, developed by TDK (formerly InvenSense), is yet another 6-axis IMU utilized in Pixhawk 4 and other flight controllers. It shares similarities with the ICM-20689 in terms of its MEMS-based accelerometer and gyroscope configuration. The ICM20602 is known for its fast response time, low noise levels, and high accuracy, making it well-suited for applications requiring real-time motion tracking (TDK InvenSense. (n.d.)).

The importance of these IMUs in the Pixhawk 4 lies in their critical role in the flight control system. As part of the sensor suite on the flight controller board, they continuously measure the drone's linear acceleration and angular velocity, providing crucial data on its position, orientation, and motion. This information is essential for

various flight control algorithms, including attitude estimation, stabilization, and navigation.

The flight control algorithms on the Pixhawk 4 utilize the data from these IMUs to calculate the drone's attitude (roll, pitch, and yaw angles) and make necessary adjustments to the motor outputs to maintain stability and respond to pilot commands accurately. Moreover, these IMUs enable advanced flight modes, such as altitude hold and position hold, by accurately tracking the drone's vertical motion and maintaining a steady position relative to the ground.

2.3.2.2 Magnetometer

The Pixhawk 4 controller by Holybro uses a magnetometer sensor known as IST8310. This sensor is commonly used in drones due to its high precision and low cost. It has an accuracy of ±1.5 μT and a range of up to 800 μT (Holybro. (n.d.)).

The purpose of the magnetometer in the Pixhawk 4 is to measure the magnetic field of the Earth. This information is then used to determine the orientation of the drone. The magnetometer works together with the accelerometer and gyroscope to provide a more accurate estimate of the drone's orientation.

Apart from determining orientation, the magnetometer is also used in the Pixhawk 4 to detect magnetic anomalies. These anomalies are often caused by metal objects such as buildings, power lines, and cars. The magnetometer can detect such anomalies and help the drone avoid them. The magnetometer is an essential component of the Pixhawk 4 flight controller and is crucial for safe and reliable flight. It offers many benefits, including improved orientation estimation, detection of magnetic anomalies, and compensation for magnetic interference.

The Pixhawk 4 also supports the ICM-20948 sensor, which has a slightly higher accuracy than the IST8310 sensor. However, the ICM-20948 is more expensive. The choice of which sensor to use depends on the specific application. For applications that require high accuracy, the ICM-20948 is a good choice. For more cost-sensitive applications, the IST8310 is a good option.

2.3.2.3 Barometer

Pixhawk 4 uses a MEMS barometer, which is a small and lightweight sensor that measures atmospheric pressure. It estimates the altitude of the drone by detecting the decrease in atmospheric pressure with increasing altitude. The barometer used in Pixhawk is typically a high-precision and low-cost MS5611 sensor that has a range of up to 1100 hPa and an accuracy of ±0.2 hPa (Farnell. (n.d.); TDK InvenSense. (n.d.)).

To estimate the altitude of the drone accurately, Pixhawk uses both the GPS and the barometer. While the GPS provides the horizontal position of the drone, the barometer provides its altitude. The data from both sensors are combined to produce a more precise estimate of the drone's altitude. Additionally, the barometer in Pixhawk compensates for changes in atmospheric pressure to maintain the accuracy of the altitude estimate. This is crucial because changes in atmospheric pressure can affect the accuracy of the GPS.

The barometer is a vital component of the Pixhawk flight controller, ensuring safe and reliable flight. It plays a crucial role in estimating the drone's altitude and compensating for atmospheric pressure changes.

2.3.2.4 GPS

Pixhawk is equipped with the M8N GPS module, an exceptional high-precision, low-power GPS receiver. Its compatibility with the Pixhawk flight controller makes it a reliable source for accurate positioning data in applications ranging from autonomous flight to navigation and mapping.

The M8N GPS module boasts features that make it a preferred choice for Pixhawk, including:

- High precision: With an accuracy of up to 0.6 meters, the M8N GPS module delivers exceptional precision for applications that require precise positioning.
- Low power consumption: Its low power consumption makes it ideal for battery-powered applications.
- Wide range of supported GNSS constellations: The M8N GPS module supports various GNSS constellations, including GPS, GLONASS, Galileo, and BeiDou, ensuring accurate positioning data in any environment.

While other GPS modules like the M9N GPS module can also be used with Pixhawk, the M8N GPS module is highly recommended for applications that require high precision positioning (Holybro. (n.d.)).

CHAPTER THREE: METHODOLOGY

3.1 Research Framework

The thesis is started from literature review to find research gap. Based on the research gap, problem statement is developed which helps in formulation of objectives. The framework of this thesis is as per below flowchart:

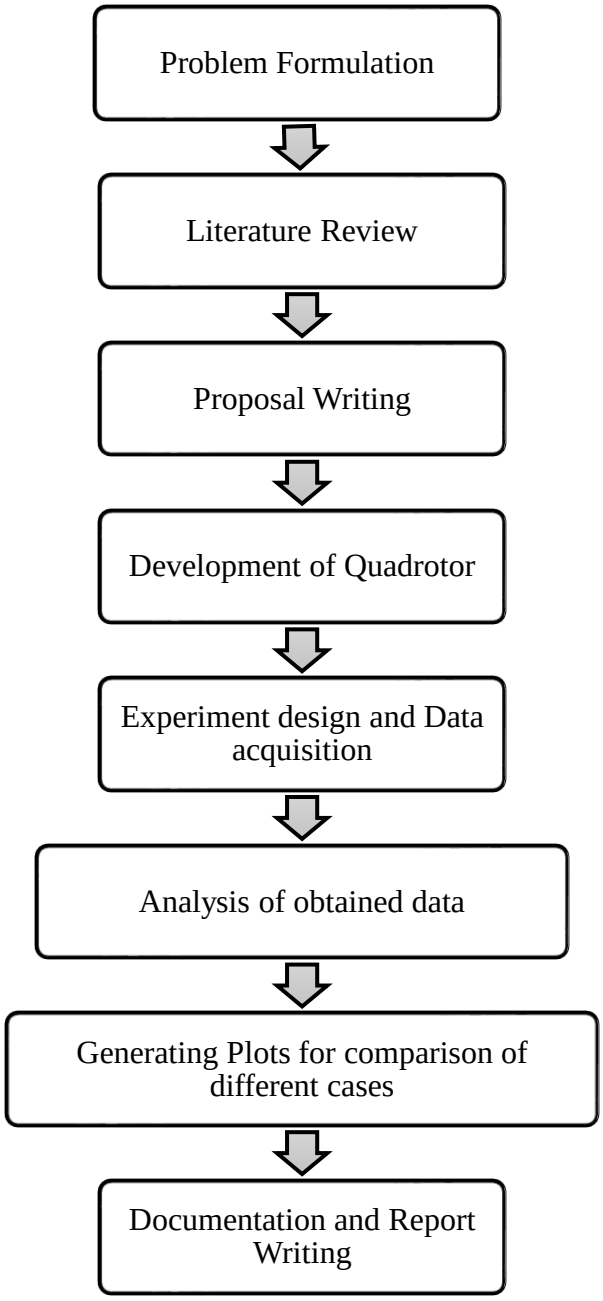

Figure 3.1: Workflow diagram of research methodology

3.1 Problem Formulation

During the problem formulation stage of the research, different ideas were analyzed and assessed for the value addition it would had on the society as a whole with minimal added cost. Among different ideas, concept of delivering the emergency supplies and making other commercial delivery seemed novel. Many of the researcher were working on the problem in these recent years.

3.1 Literature Review

Reviewing the articles and journal papers related to the cable suspended payload system provided insights into the current development in this field. Literature review on the experimental evaluation of payload induced oscillations of an unmanned rotorcraft was done extensively to cover as much literature as practically possible, in order to get the overall idea about the development in this field. Different books, research papers, journals and internet articles and websites has been consulted in this process.

3.2 Proposal Writing

The proposal was submitted to our Program Coordinator Prof Dr. Laxman Poudel sir for the necessary assignment of Supervisor in line with the research subject and objective. Proposal Writing formally established the topic of research as supervisors were assigned after that.

3.3 Development of Quadrotor

A Quadrotor system was developed with an onboard Pixhawk controller. Due to the wide use case scenario and easy assembly quadrotor was constructed on a Generic S500 frame in X configuration with Pixhawk4 as an onboard controller. It was equipped with 1045 propellers and 980kv B2212 BLDC (Brushless Direct Current) motor for propulsion. The required power for propulsion was provided with 40C 3700mah, a 3-cell battery pack. Brushless DC needs ESC to vary the power output as per the signal input for a controlled motor operation. Therefore, each motor was controlled using 30A ESC to provide the quadrotor.

3.4 Experiment Design and Data Acquisition

A quadrotor with a cable-suspended payload experiences payload inertia while accelerating, decelerating, and with altitude change. This induces destabilizing effect

on the quadrotor due to the force transmitted via the suspension cable. By understanding the quadrotor response and behavior under different flight conditions with a tethered payload, an improved payload delivery system can be achieved.

This research was focused on experimental evaluation and study of payload-induced oscillation on two pre-defined autonomous mission paths for different tethered payloads attached to a quad frame about CoG (center of gravity) with disturbing conditions set along the mission path. Pixhawk4 controller running the open-source PX4 autopilot system was used on this quadrotor, as this has wide use in academia. Furthermore, by using an autopilot suitable for much larger UAVs, this entire system can be transferred onto a larger platform for outdoor missions or heavy payload delivery applications by developing dimensionless quantities

Two non-dimensional parameters considered for this experiment are defined below:

$$Non-dimensionalmass(NDM)\ \mathrm{M} = \frac{\text{mass of the payload}(M_p)}{\text{mass of quadrotor}(M_Q)}$$

$$\text{Non}-\text{dimensional length(NDL)}\ \mathrm{L} = \frac{\text{length of tether from CoG}\ (\mathrm{L_c})}{\text{length of quadrotor arm}\ (\mathrm{L_{qa}})}$$

$$\text{Normalized time} = \frac{\text{time in second}}{\text{Total Time to Complete the Misison}} = \frac{\mathrm{t}}{\mathrm{T}}$$

Different autonomous flight missions were carried out with varying payload masses with different cable length. For storage of the mission flight log data, an SD card was set up in the Pixhawk controller SD card slot. The Pixhawk records its data in .ULOG format, which were later post-processed to get different .CSV files containing flight information.

Different cases along pre-defined autonomous paths were evaluated for the study. And each test cases were performed twice for the purpose of Validation.

Table 3.1: Sample Test Cases

Mission 1 (P_1)	L_0	1) M_0 and L_0
	L_1	2) M_1 and L_1
		3) M_2 and L_1
	L_2	4) M_1 and L_2
		5) M_2 and L_2

	L_3	6) M_1 and L_3
		7) M_2 and L_3
	L_4	8) M_1 and L_4
		9) M_2 and L_4
	L_5	10) M_1 and L_5
		11) M_2 and L_5
Mission 2 (P2)	L_0	12) M_0 and L_0
	L_1	13) M_1 and L_1
		14) M_2 and L_1
	L_2	15) M_1 and L_2
		16) M_2 and L_2
	L_3	17) M_1 and L_3
		18) M_2 and L_3
	L_4	19) M_1 and L_4
		20) M_2 and L_4
	L_5	21) M_1 and L_5
		22) M_2 and L_5

3.4 Analysis of the Obtained data

The recorded data was analyzed for oscillation in the vehicle's altitude and different control axis using a MATLAB program. Analysis were done based on the plots of different cases of autonomous mission flight. MATLAB plot for different cases of altitude, speed, payload mass, and cable length were evaluated and associated vibration of the UAS as recorded with accelerometer and gyroscope was also evaluated. Fast Fourier Transform (FFT) was performed on thus obtained data to evaluate the dominant vibration and oscillations frequency. After evaluating the frequencies, corresponding Power Spectrum Density (PSD) was analyzed to obtained result, thus assessing the performance of the quadrotor under various different cases.

3.5 Generating Plots for comparison of different cases

Different plots related to different cases of the autonomous flight of the UAS were generated to make a comparative study of the effect of varying cable length and payload mass on the vehicle oscillation. Thus obtained results were compared for different cases, such as, effect of increasing cable length, effect of increasing payload mass, effect of change in mission path etc.

Thus, obtained results were verified before moving towards any conclusion. Primarily the validity of the developed model was checked by cross-referencing with analytical solution of the system, and validating the trend of the data with similar nature of work.

CHAPTER FOUR: EXPERIMENT DESIGN

4.1 Experimental Setup

The experiment was performed in an outdoor environment, and all the data were taken during the morning time when there was negligible wind gust affecting the quadrotor dynamics. In order to isolate the effect of payload on quadrotor dynamics and performance, a flight without any suspended payload was performed. This helped to isolate and visualize the effect of varying payload mass with different cable lengths. Furthermore, all the flight for a particular mission was started at the exact location to introduce uniformity in data.

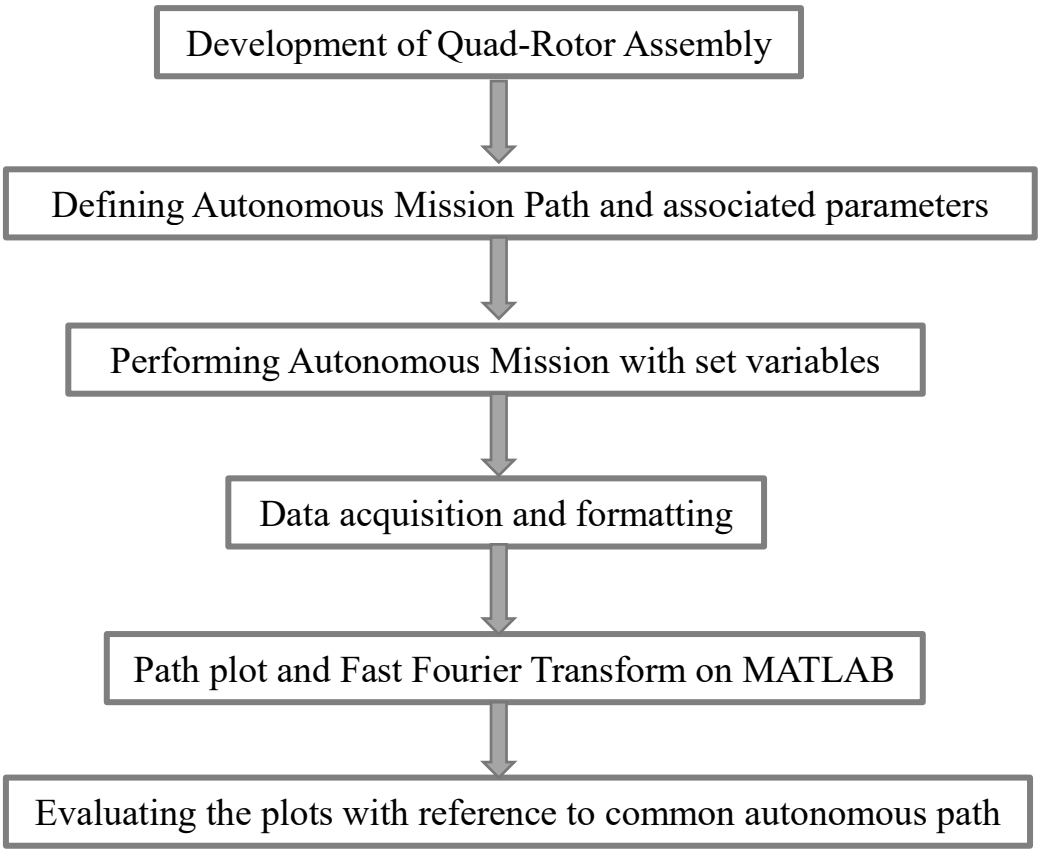

Figure 4.1: Experimental methodology

4.1.1 Quadrotor Assembly

A quadrotor model was assembled with an onboard Pixhawk controller. Due to the wide use case scenario and easy assembly quadrotor was constructed on a Generic S500 frame in X configuration with Pixhawk4 as an onboard controller. It was equipped with 1045 propellers and 980kv B2212 BLDC (Brushless Direct Current) motor for propulsion. The required power for propulsion was provided with 40C 3700mah, a 3-cell battery pack. Brushless DC needs ESC to vary the power output as per the signal input for a controlled motor operation. Therefore, each motor was controlled using 30A ESC to provide the quadrotor.

Figure 4.2: Final quadrotor assembly

The autonomous mission is carried out with the use of the TELEM1 port on the Pixhawk 4 module, which communicates wirelessly with a ground station for monitoring and changing any parameters during the flight. Qgroundcontrol, an open-source Pixhawk-compatible ground station, was used as the ground control station for this autonomous mission and quadrotor mission planning and calibration. For the position and path estimation, a GPS module is needed; Pixhawk4 GPS module was used in conjunction with Pixhawk 4 onboard IMU and barometric sensor to estimate the altitude.

Using the standard thrust of 780 grams per motor from the specification of the B2212 BLDC motor with a 1045, 1o inch propeller, the total available thrust for the quadrotor was 3120 grams. As a rule of thumb, the quadrotor can carry half the weight of the total thrust without affecting its maneuverability. As the total weight of the assembled quadrotor was 1.350 kg, an extra 0.20 kg of payload can be attached for this assembly. A standard weight of 0.10 kg was chosen as the payload. The mass of the suspension cable was negligibly small; thus, we do not consider its weight during this analysis.

Table 4.2: Quadrotor assembly and its payload weight

Quadrotor weight	1.350 kg
With a payload 0.1 kg	1.450 kg
With a payload 0.2 kg	1.550 kg

Figure 4.3: Quadrotor with 0.1 kg payload

4.1.2 Mission Paths

For the uniformity in data, two standard missions were developed for the quadrotor's autonomous flight. For the ease of operation and wider flexibility over the parameter control, qgroundcontrol was used to draw the following mission profiles. Also, the path parameters are set on the quadrotor mission paths. For the simplicity of analysis and to cover all possible quadrotor motion profile, the mission paths were made as simple as possible including all range of quadrotor motion.

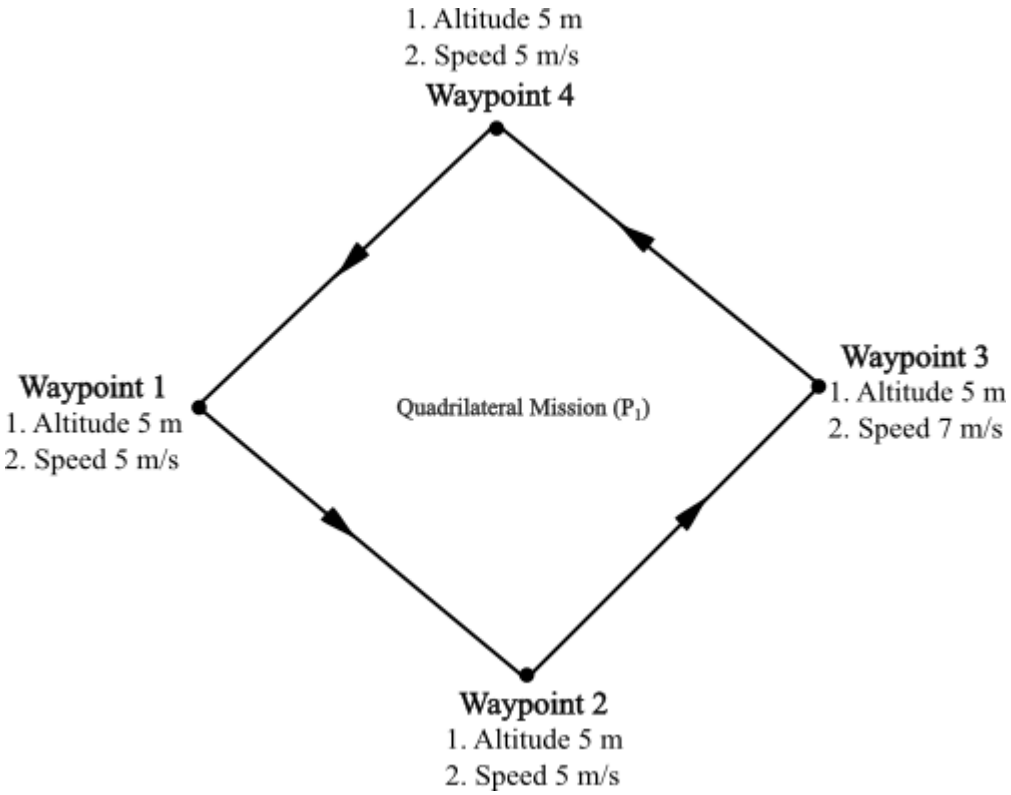

Figure 4.4: Quadrilateral mission path (P_1)

1. *Quadrilateral mission path (P_1):* For the simplicity of analysis and eliminating unnecessary factors in analysis, a simple quadrilateral mission path was developed in qgroundcontrol. The quadrotor was set to fly at an altitude of 5 meters above ground at a default speed of 5 m/s on all paths except for the path from waypoint 3 to waypoint 4, where the flying speed is set at 7m/s. This was set to analyze the effect of change in speed of the vehicle.
   Path Varibles for the Quadrilateral mission profile is as given below

Table 4.3 Path Variables for Quadrilateral Mission Path (P_1)

WayPoint	**Altitude**	**Speed**
Waypoint 1	5 m	5 m/s
Waypoint 2	5 m	5 m/s
Waypoint 3	5 m	7 m/s
Waypoint 4	5 m	5 m/s

2. *Triangular mission path (P_2):* Another triangular mission path was developed in qgroundcontrol. In this case, speed along all the mission waypoints was set constant at 5m/s, while altitude was changed from 5 m to 10m on waypoint 2 of this path to analyze the effect of change in altitude on vehicle response.

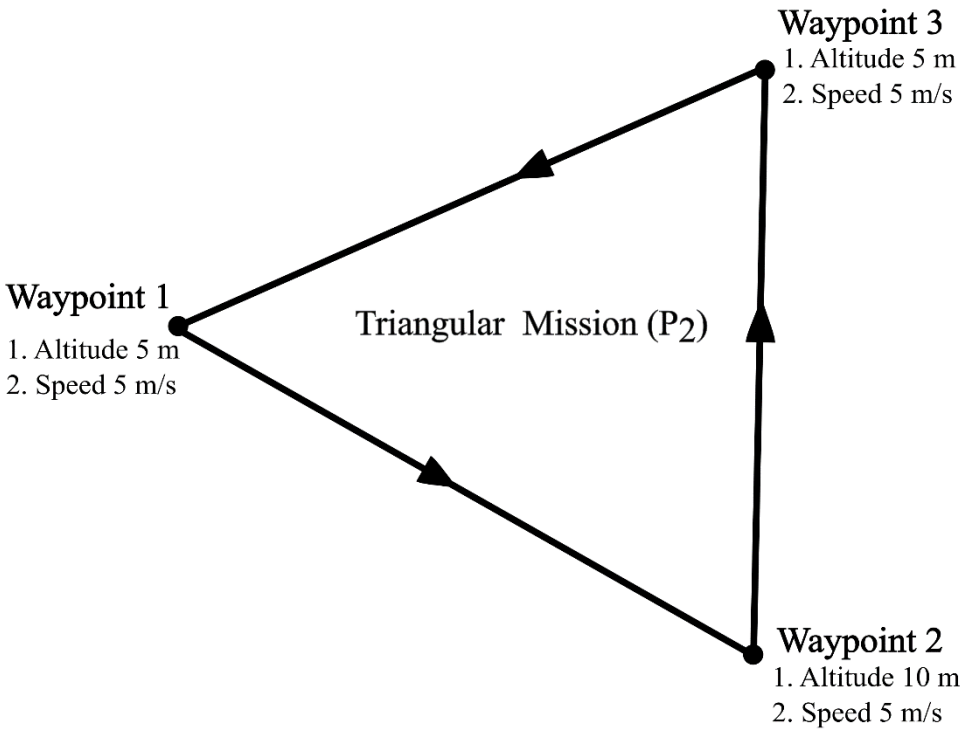

Figure 4.5: Triangular mission path (P_2)

Table 4.4 Path Variables for Triangular Mission Path P_2

WayPoint	**Altitude**	**Speed**
Waypoint 1	5 m	5 m/s
Waypoint 2	15 m	5 m/s
Waypoint 3	5 m	5 m/s

For these two mission profiles, the 22 distinct test case scenarios were experimentally evaluated.

4.2 Test Cases

For this experimental study three different cable length were used to suspend two different kind of mass from the quadrotor. Thus, we can define nondimensional parameters for each cable length and each mass. And, we can define each mission case according to the nondimensional parameters involved.

For ease of convention, non-dimensional mass and nondimensional length parameters are defined separately.

Non-dimensional mass

$$\mathrm{M}_0 = \frac{\text{mass of the payload}(M_p)}{\text{mass ofquadrotor}(M_Q)} = \frac{0\ \text{kg}}{1.35\ \text{kg}} = 0$$

$$\mathrm{M}_1 = \frac{\text{mass of the payload}(M_p)}{\text{mass ofquadrotor}(M_Q)} = \frac{0.1\ \text{kg}}{1.35\ \text{kg}} = 0.07407$$

$$\mathrm{M}_2 = \frac{\text{mass of the payload}(M_p)}{\text{mass ofquadrotor}(M_Q)} = \frac{0.2\ \text{kg}}{1.35\ \text{kg}} = 0.14815$$

Non-Dimensional Length

$$\mathrm{L}_0 = \frac{\text{length of suspension cable from CoG}(\mathrm{L}_c)}{\text{length of quadrotor arm }(\mathrm{L}_{qa})} = \frac{0\ m}{0.5\ m} = 0$$

$$\mathrm{L}_1 = \frac{\text{length of suspension cable from CoG }(\mathrm{L}_c)}{\text{length of quadrotor arm }(\mathrm{L}_{qa})} = \frac{0.3\ m}{0.5\ m} = 0.6$$

$$\mathrm{L}_2 = \frac{\text{length of suspension cable from CoG}(\mathrm{L}_c)}{\text{length of quadrotor arm }(\mathrm{L}_{qa})} = \frac{0.4\ m}{0.5\ m} = 0.8$$

$$\mathrm{L}_3 = \frac{\text{length of suspension cablefrom CoG }(\mathrm{L}_c)}{\text{length of quadrotor arm }(\mathrm{L}_{qa})} = \frac{0.5\ m}{0.5\ m} = 1.0$$

$$\mathrm{L}_4 = \frac{\text{length of suspension cablefrom CoG }(\mathrm{L}_c)}{\text{length of quadrotor arm }(\mathrm{L}_{qa})} = \frac{0.7\ m}{0.5\ m} = 1.4$$

$$\mathrm{L}_5 = \frac{\text{length of suspenion cable from CoG }(\mathrm{L}_c)}{\text{length of quadrotor arm }(\mathrm{L}_{qa})} = \frac{1\ m}{0.5\ m} = 2$$

$$Normalized\ time = \frac{time\ in\ second}{Total\ Time\ to\ Complete\ the\ Misison} = \frac{t}{T}$$

Table 4.5 Test Cases in Experiments

Mission	**Cable Length**	**Test Case number and corresponding Non-Dimensional Term**
Mission 1 (P_1)	L_0	1) $M_0 = 0$ and $L_0 = 0$
	L_1	2) $M_1 = 0.07407$ and $L_1 = 0.6$
		3) $M_2 = 0.14815$ and $L_1 = 0.6$
	L_2	4) $M_1 = 0.07407$ and $L_2 = 0.8$
		5) $M_2 = 0.14815$ and $L_2 = 0.8$
		6) $M_1 = 0.07407$ and $L_3 = 1$

	L_3	7) M_2= 0.14815 and L_3= 1
	L_4	8) M_1= 0.07407 and L_4 = 1.4
		9) M_2= 0.14815 and L_3= 1.4
	L_5	10) M_1= 0.07407 and L_5 = 2
		11) M_2= 0. 14815 and L_5 = 2
Mission 2 (P2)	L_0	12) M_0 = 0 and L_0 = 0
	L_1	13) M_1 = 0.07407 and L_1 = 0.6
		14) M_2 = 0.14815 and L_1 = 0.6
	L_2	15) M_1 = 0.07407 and L_2 = 0.8
		16) M_2 = 0.14815 and L_2 = 0.8
	L_3	17) M_1= 0.07407 and L_3= 1
		18) M_2= 0.14815 and L_3= 1
	L_4	19) M_1= 0.07407 and L_4 = 1.4
		20) M_2= 0.14815 and L_3= 1.4
	L_5	21) M_1= 0.07407 and L_5 = 2
		22) M_2= 0. 14815 and L_5 = 2

CHAPTER FIVE: RESULTS AND DISCUSSIONS

The performance of a quadrotor can vary significantly depending on the segment of the flight. For example, during takeoff, the quadrotor may exhibit different behavior than during cruising or landing. During the takeoff segment, the quadrotor must generate enough thrust to overcome its weight and lift off the ground. This requires a high level of power from the rotors, which can lead to increased vibration and decreased efficiency. Once the quadrotor is airborne, the focus shifts to maintaining a stable hover. This requires precise control of the rotors, as even small imbalances can cause the quadrotor to drift, and with tethered payload, it becomes even more challenging to control the vehicle. In the cruise segment, the quadrotor typically flies at a constant speed and set altitude. This is the most efficient segment of the flight, as the quadrotor is not required to generate as much thrust. However, even during the cruise, during the turning of the quadrotor from mission to mission, it has to change its direction and maintain stability. Then Finally, during the landing segment, the quadrotor must decelerate and touch down gently. This requires precise control of the rotors; as even small errors can lead to a crash.

By analyzing the performance of the quadrotor according to the specific segment of the flight, it is possible to gain a more detailed understanding of its behavior and capabilities. This can be useful for optimizing the quadrotor's performance and improving its overall efficiency. Additionally, by analyzing the performance of the quadrotor according to the segment of the flight, it is possible to identify any potential issues or areas for improvement, which can help to enhance the safety and reliability of the quadrotor.

In this study, all different plots of pitch, roll, yaw, altitude, and other variables are plotted against a non-dimensional form of time, this is done in order to harmonize the curves irrespective of start and end time for the autonomous mission as the start time of each mission may vary due to multiple reasons. Also, only the most significant data were plotted in order to avoid clutter and have a clearer picture of the characteristics of the quadrotor under the tethered payload condition. All the characteristics and performance of the quadrotor are analyzed with reference to the following different segments of the flight:

1) Take-off and Climb
2) Trajectory flight
    a) Cruise along the straight path
    b) Corner and turn
3) Landing

The following figure below helps visualize the flight segment with reference to the vehicle altitude. Waypoint 1 is situated at 0.18 on the non-dimensional time axis of the plot. During the cruising phase of the flight, the vehicle loses a certain height when yawing around at mission waypoints. Also, the vehicle's return to launch is usually initiated at a height lower than that of the waypoint set altitude, this is because the vehicle decelerates and loses its height before reaching the first waypoint for landing, which is characteristic of the Pixhawk controller.

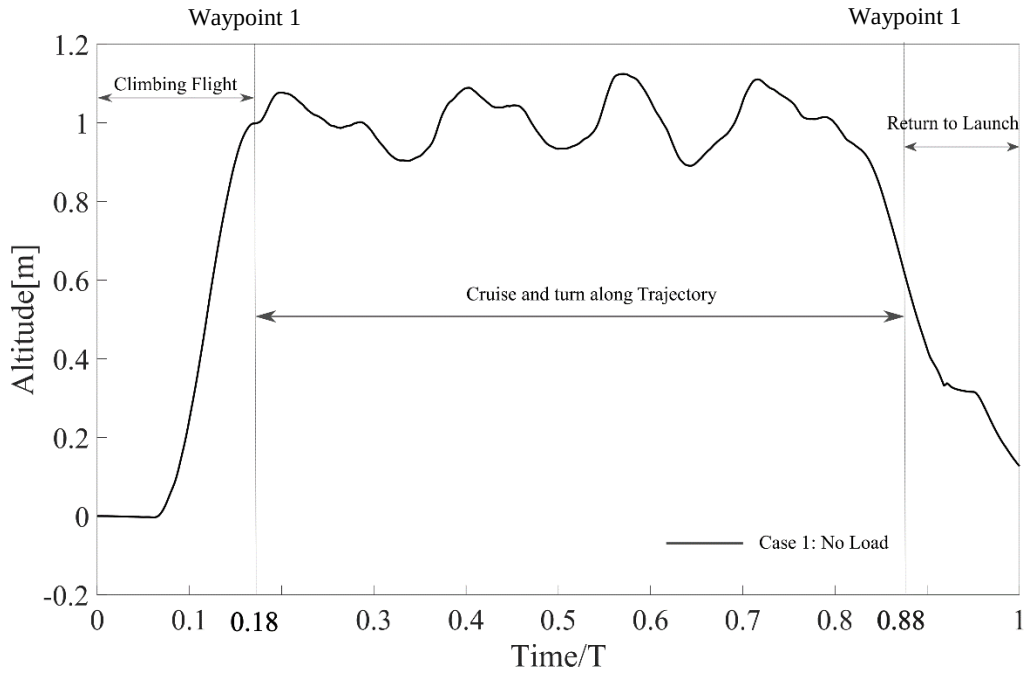

Figure 5.1: Altitude vs time plot showing different phases of flight for no load

5.1 Take-off and Climb

As shown in Figure 5.1, this flight segment ranges from when the quadrotor is at the ground and is just ready to take off for the climb to reaching waypoint 1 with the set altitude value. After which a Cruise flight will ensue. During the initial start and takeoff of the UAS in an autonomous mission, it initially tries to compensate for the instability in vehicle takeoff, by adjusting the UAS attitude to maintain the stability of the flight.

Upon the analysis of the data from the experiment, it is found that there is notable fluctuation of the pitch and roll of the vehicle, while vehicle yaw remains essentially similar for the most part of the autonomous path.

5.1.1 Effect on Pitch

In the following Figure 5.2, shows, the rectangular section A shows the Variation of the Pitch angle with time on mission path P_1 during the take-off and Climbing phase for the quadrotor. In Figure 5.3, we can see that there is a significant increase in pitching oscillation with the increase in payload mass. The line representing the no-load condition of the flight is comparatively oscillation free apart from the necessary pitching of the quadrotor for the autonomous mission path. However, in case 6, the increase in mass and cable length of a half meter has added disturbances to the system, which need to be balanced by the controller before starting the cruising segment of the flight.

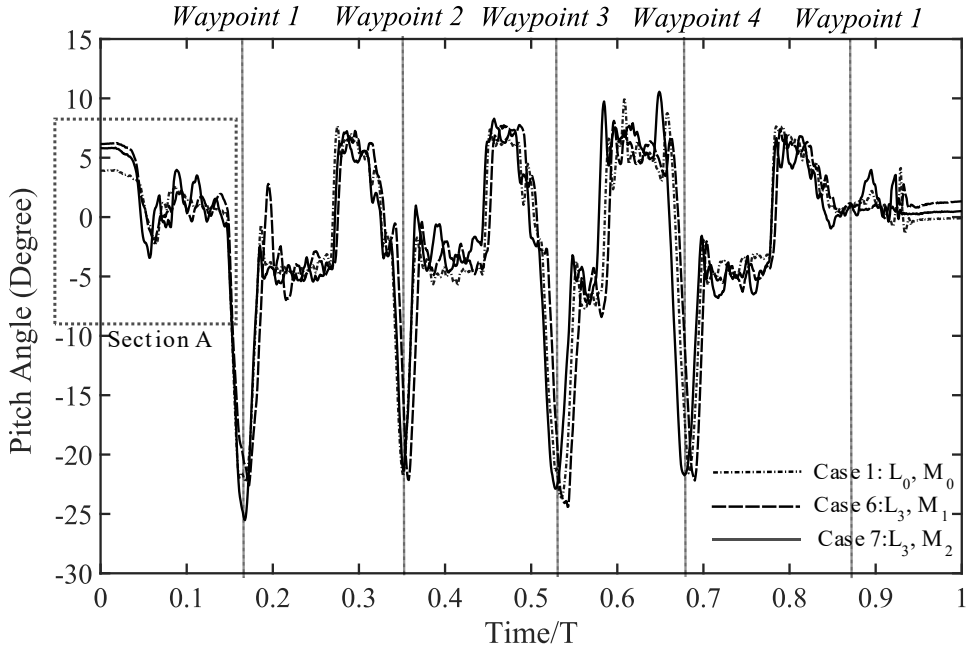

Figure 5.2 Variation of pitch angle with time on mission path P_1 with Section-A highlighting the take-off or climb of segment of mission

In the figure 5.3, the pitch variation for the quadrotor with a suspended load condition is illustrated along with the peak value of the pitch angle in both negative and positive spectra. Although there is fluctuation in pitch even on no load condition to attain the initial take off balance of the UAS, it progressively increases with increase in added mass on the cable length. In this particular graph, we can compare the effect of additional payload on the vehicle pitching performance during the take-off phase of the flight.

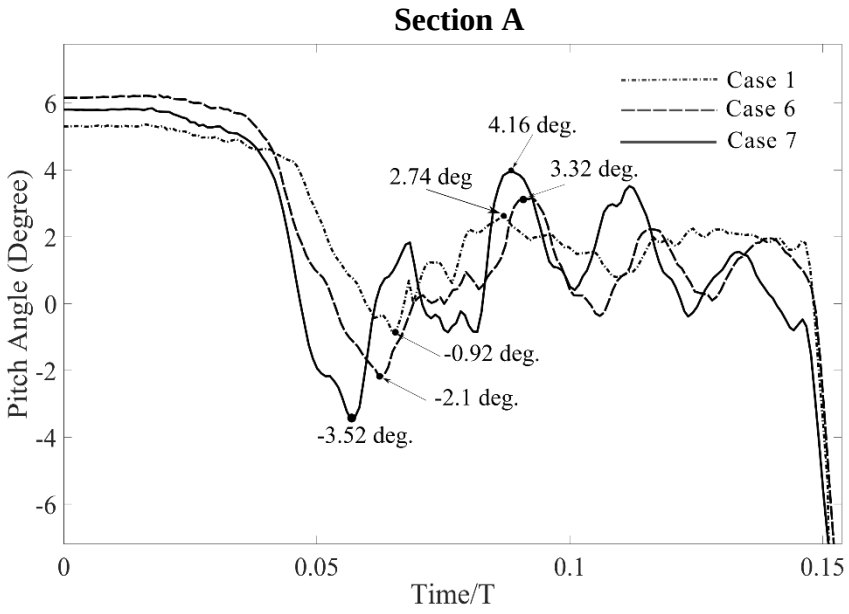

Figure 5.3: Variation of pitch angle with time on Section-A

In figure 5.3, it can be seen that after the initial takeoff of the quadrotor, the quadrotor tries to control the disturbances by pitching up and down using the ESC and motor thrust power. Furthermore, the range of initial pitching adjustment increases with an increase in tethered payload mass. Initially, with no load condition the pitching correction is between +2.74 deg to -0.92 deg with a range of 3.68 deg. But with case 6, with 0.1 kg payload suspending on a 0.5 m string, the pitching correction fluctuates between +3.32 deg to -2.1 deg with a range of 5.42 deg. Furthermore, with case 7, 0.2 kg payload suspended with 0.5 m string, the pitching correction increases drastically to a range of 7.68 deg between +4.16 deg to -3.52 deg.

So, in comparison with the no load condition, the pitching correction of the quadrotor increases by 47.28 % in case 6. Similarly, the pitching correction increases by nearly 108.69% during the initial takeoff phase of the flight. Also, with the increased mass

from 0.1 kg to 0.2 kg, the pitch angle fluctuation increases by 41.69% during the take-off phase of the autonomous mission. This increase in pitching correction may been occurred due to the pull that the payload exerts on the quadrotor, since during the initial takeoff of the

5.1.2 Effect on Roll

Similar to the effect of payload mass and cable length pitch, another translational oscillation profile of interest is the effect of payload mass and tether length on the roll angle of the vehicle during the initial take-off stage of the quadrotor. The following Figure 5.4, shows the roll angle variation of the quadrotor with reference to the normalized time.

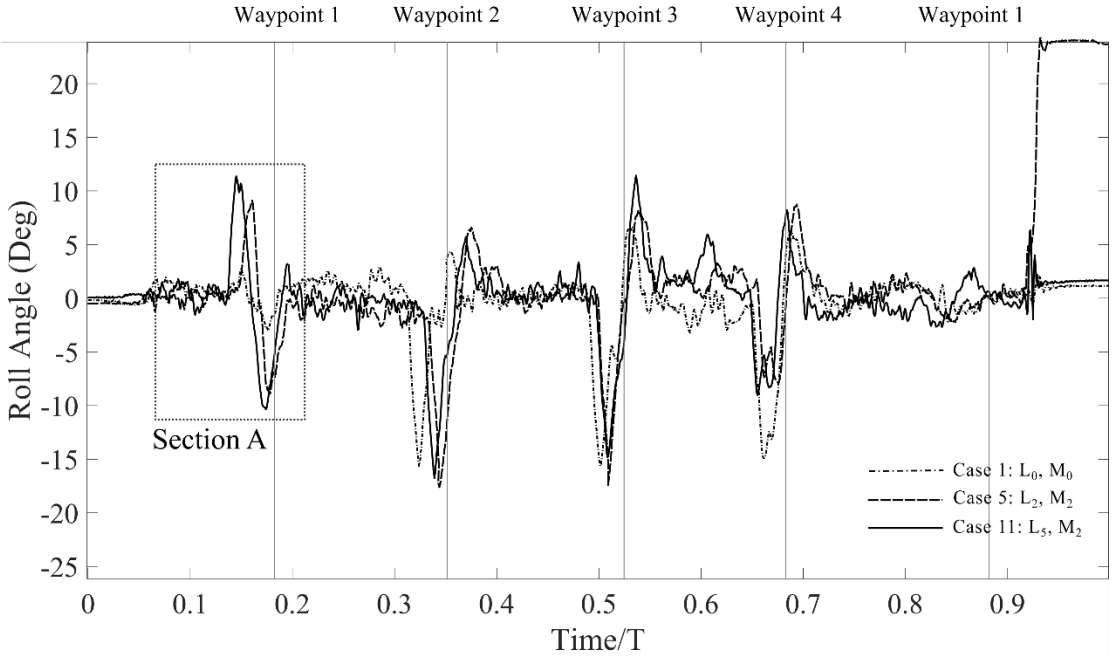

Figure 5.4: Roll angle variation over time with Section-A highlighting of take-off/ climb segment of mission

In this figure, we can see a significant fluctuation in the roll angle of the quadrotor when it is attached to a tethered payload when compared to no load condition. The fluctuations are caused by the pull of the tethered payload, which increases with increased payload mass. The following Figure 5.5 depicts the roll angle variation during the initial takeoff phase of the quadrotor.

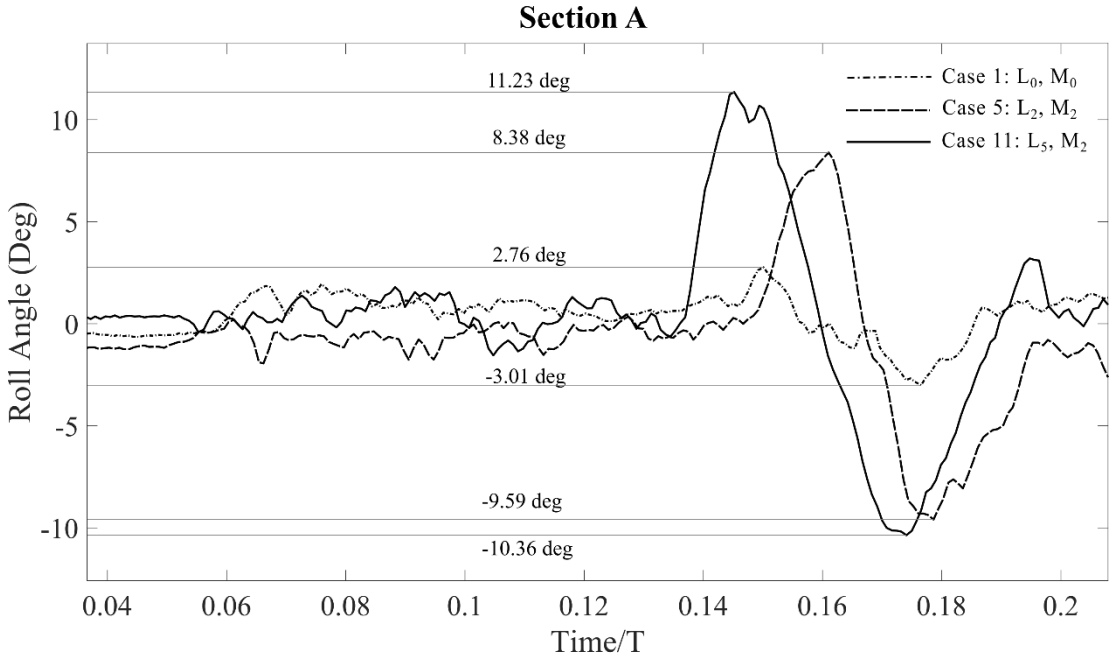

Figure 5.5: Effect of tether length on roll angle variation during Section-A

To illustrate the effect of increasing tether length, case 5 and case 11 are plotted along with the no-load condition. We can see from Figure 5.5 that, in comparison to the no load condition, case 1, the successive cases with M_2 demonstrate increasing fluctuation in roll angle. In case 1, the roll angle of the quadrotor fluctuates with a range of 5.77 deg, however with tethered payload, the roll angle fluctuation increases significantly with increasing tether length. With the increase of cable length from 0.5m to 1m, the roll angle fluctuation range increases by 20.14 %. This increase in fluctuation may have been caused by the increased moment of the suspended mass on the quadrotor due to an increase in tether length. Another interesting thing to note is the time period of oscillation of the roll angle increases with an increase in cable length, which is due to the fact that the tethered payload behaves very much similarly to the simple pendulum when suspended on a single point from the quadrotor.

Similar to the tether length, the payload mass also has an effect on the roll angle fluctuation during the takeoff phase of the flight. The following Figure 5.6 compares the roll angle of two payload masses, with 1m cable length in comparison to the no-load condition. The increase in payload has an effective increase of 22.8% increase in

roll angle fluctuation. This again is due to the increased payload pull that the quadrotor experiences with the increase in payload mass. However, with the similar length of the tether, both pitching oscillations have nearly the same period of oscillations.

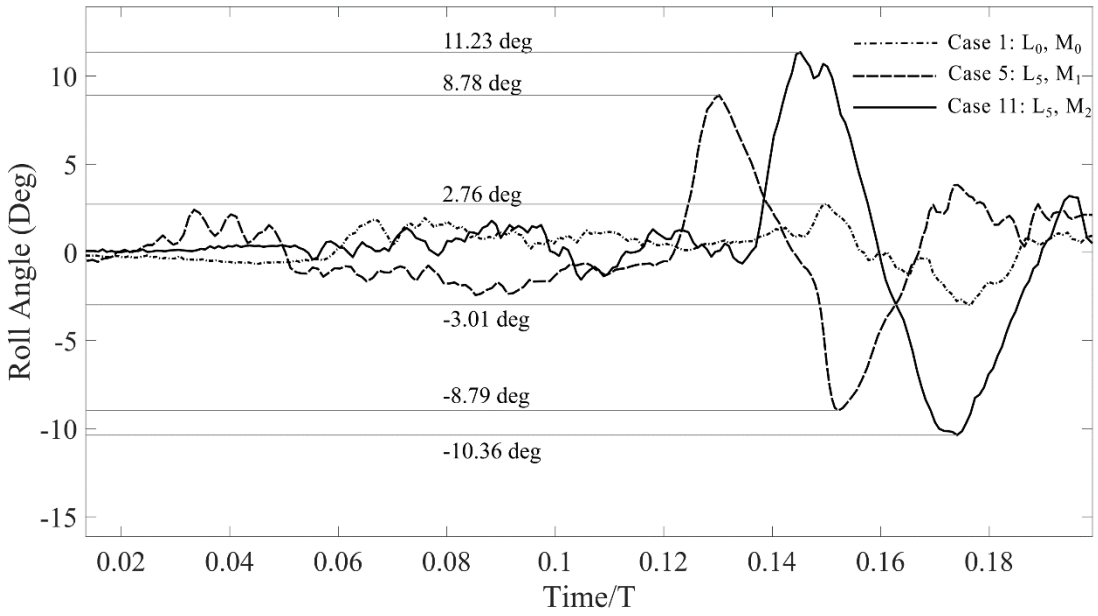

Figure 5.6: Effect of payload mass on roll angle variation with payload mass during section A

5.2 Trajectory Flight

The quadrotor moves about the planned mission paths, which are defined in the previous chapter after it takes off from the ground and reaches waypoint point 1. From here on, the quadrotor cruises along the straight line of the path and makes necessary turns along the way. During this cruising phase, the attitude (yaw, pitch, roll) of the vehicle characterizes the quadrotor movement along the mission profile at the set level altitude.

In the following Figure 5.4, the we can see the variation of pitch of the quadrotor with normalized time. During the trajectory along the mission path line, the quadrotor cruises along a straight path between the waypoints and performs a turn around the corner that is each waypoint of the mission. The figure highlights the section B, which is the cruise flight along the waypoint 2 and waypoint 3. We can see that the pitch angle of the quadrotor has fluctuations along the entire range of cruise flight as well. This is primarily because of the nature of the Pixhawk controller, as we can see from the Figure

5.1 the controller slows the quadrotor down during the corner yaw and then picks up the speed along the cruise. Since the quadrotor loses its altitude during the yaw, the

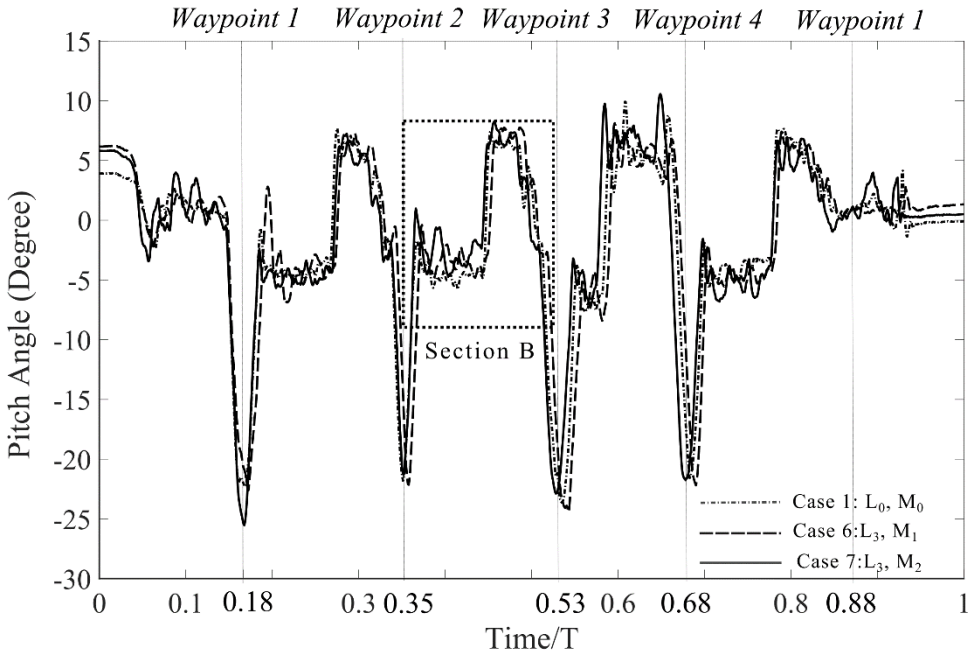

Figure 5.7: Variation of pitch angle with time on mission path P_1 with straight-line cruise section-B highlighted

quadrotor pitches up and tries to gain the set altitude during the remaining phase of the cruising flight.

5.2.1 Cruise along a Straight Line

During any autonomous mission, the quadrotor is mostly cruising along a straight path. This makes the straight-line cruise an important area to study in order to make the quadrotor mission efficient and reliable.

Similar to the take-off performance analysis of the quadrotor, the cruise performance is analyzed for pitch and roll characteristics, as the tethered payload did not show any significant influence on the yawing of the quadrotor about the vertical axis. This may have been because, the axis of the yaw is parallel to the suspension tether, due to which there are not many payload dynamics that come into play with tethered payload as well.

The cruising performance along a straight line is therefore analyzed for the following:

- Pitch angle characteristics
- Roll angle characteristics

5.2.1.1 Pitch angle characteristics

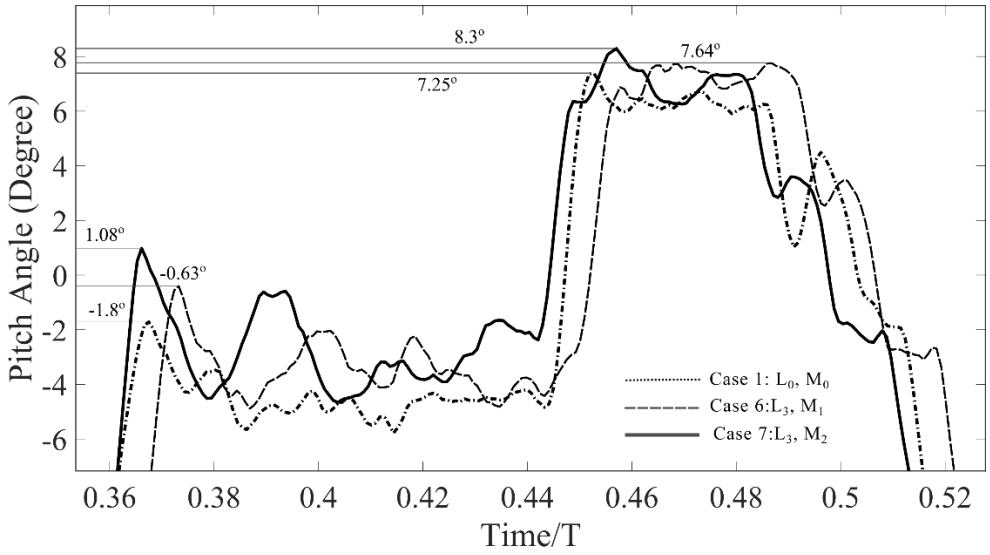

Figure 5.8: Variation of pitch angle with time on section B

Figure 5.8, highlights the straight-line cruise of the quadrotor on mission profile 1 between waypoint 2 and waypoint 3 of the flight path. We can see that during the first half of the graph, the pitch angle of the quadrotor is toward the negative end, this is because after losing height as the quadrotor slowed down during the yaw when cruising towards waypoint 3, the Pixhawk controller adjusts the altitude of the quadrotor by sudden pitch up. This causes the quadrotor to overshoot the set mission altitude, therefore the quadrotor maintains the set altitude by pitching down of the quadrotor during the initial cruising of the vehicle. After a certain time of the pitching down, it again undershoots the set mission altitude, which causes the controller to pitch up the vehicle in order to regain the flight at the mission altitude. This can be seen around the mid-section of Figure 5.8.

In Figure 5.8, the pitch angle adjustment during different mission cases are being compared. During the initial half of the figure, when the quadrotor adjusts for altitude overshoot, the pitch angle adjustment in no load condition peaks at -1.8°, however for tethered payload condition the pitching adjustment is more: -0.63° for case 6 and 1.08° for case 7. This means that the quadrotor has to make 27.1% more pitching adjustment during the initial half of the cruise for the M_2 payload compared to M_1 when suspended from the tether length of L_3.

Similarly, during the latter part of the straight-line cruise, the pitching adjustment is seen to exhibit a similar trend of higher pitch value for payload conditions, and also for an increase in payload mass. From the figure, we can see that compared to the no-load condition case 7 has to pitch up 14.24% more. Also, when compared to case 6, an increase in payload mass causes the quadrotor to pitch 8.64% more in case 7 of the quadrotor straight-line cruise. This increase in pitch is mainly attributed to the controller's characteristics to handle the increase in payload mass with more motor thrust power.

Furthermore, we can see from Figure 5.4 that this fluctuation of pitch occurs throughout the mission path during the cruising and turning phase of the flight. However, an interesting thing to note is that, between waypoints 3 and 4, the fluctuation in pitch is significantly higher than that between other waypoints. This is mainly because of the fact the speed of the quadrotor was increased from 5 m/s to 7 m/s on waypoint 3. This increase in speed causes the quadrotor to overshoot the set altitude even further.

In addition, the increase in speed also has an effect on the pitch characteristics of the UAS. To illustrate the effect of speed on the vehicle, the following Figure 5.9 shows the pitch characteristics of the quadrotor between waypoint 2 and waypoint 4.

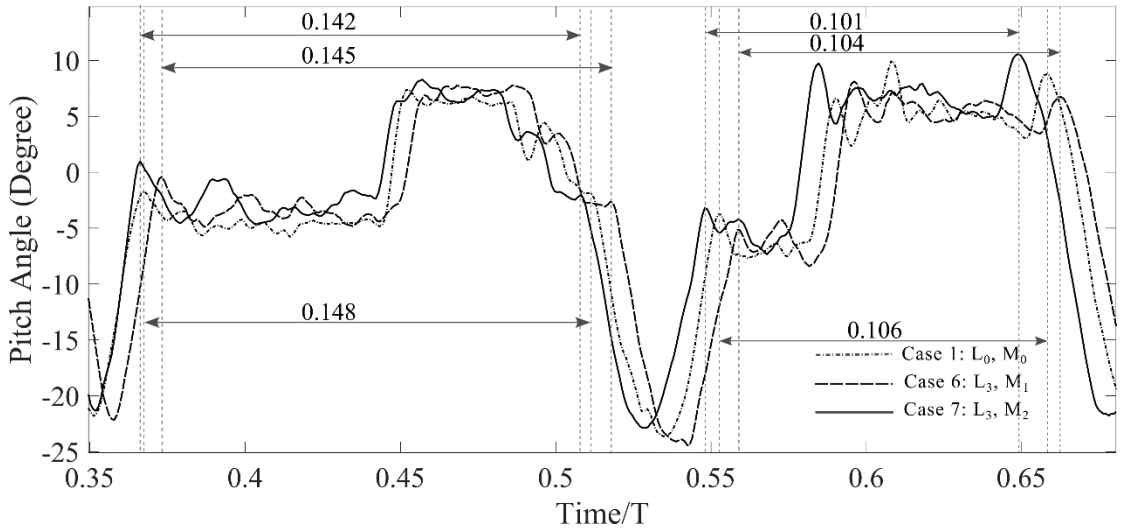

Figure 5.9: Effect of speed on cruise flight from waypoint 2 to waypoint 4

We can see from the above figure, the time period of pitch oscillation decreased by about 28.3% in all the cases, which may have been because of the reduced mission time with an increase in speed. Also, this suggests that with an increase in speed, the pitching oscillations frequency will increase proportionally.

5.2.1.2 Roll angle characteristics

Another important attitude parameter that is constantly fluctuating and adjusting along an autonomous mission path is roll angle. The roll angle of a quadrotor varies in response to the vehicle load and external disturbances. In the case of a tethered payload to the quadrotor, the tension along the tether due to payload mass, causes the rolling moment on the vehicle. Figure 5.9 shows the variation of roll angle time for case 1, case 2, and case 3. In order to study the straight-line characteristic from waypoint to waypoint, a straight-line segment is defined in section B. This section's specific roll angle characteristics are highlighted in the following Figure 5.10.

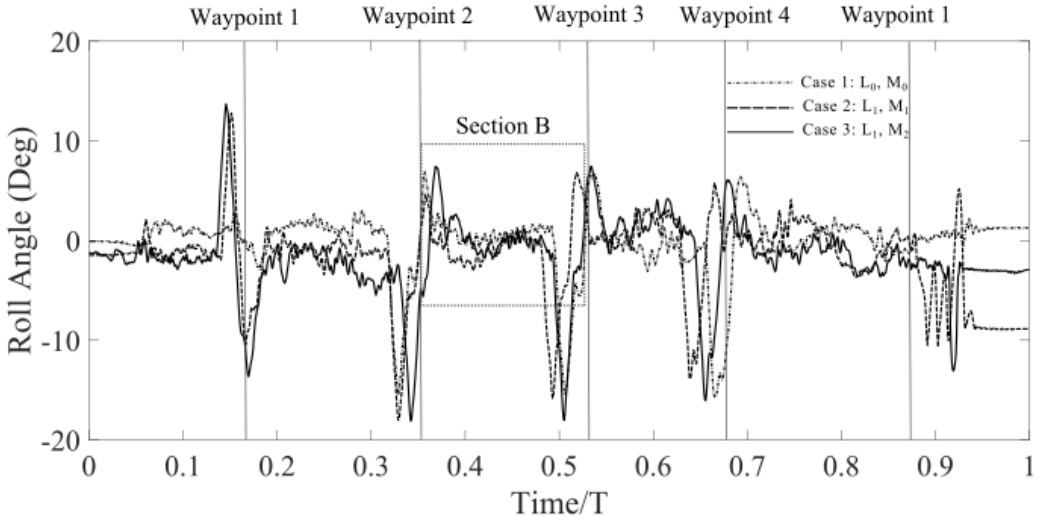

Figure 5.10: Variation of roll angle with time highlighting Section B

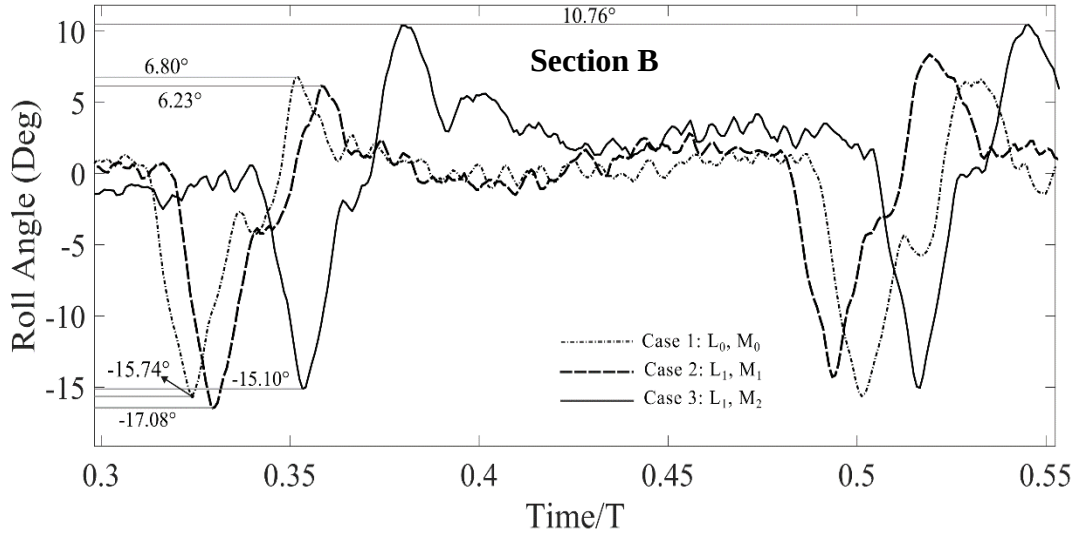

Figure 5.11: Variation of roll angle on straight-line cruise during Section-B

We can see in Figure 5.11; the roll angle of the quadrotor exhibits continuous variation during the whole flight path. Although, owing to the Pixhawk controller characteristics, all the mission paths exhibit similar roll characteristics, the amplitude of roll angle fluctuations increases with added tethered payload. Compared to the no-load condition of the rotorcraft, case 6 exhibit a marginal 3.41% increase in roll angle fluctuation. Additionally, with an increase in the mass of the payload, case 7 shows an increase of 10.93% increase in roll angle fluctuations.

5.2.2 Corner and turn During Cruise

In addition to straight-line cruising, a quadrotor has to constantly change its direction as per the instruction given to it in line with the mission waypoints. So, in order to understand the characteristics of the quadrotor around a corner, the performance of the quadrotor was evaluated for the following two types of corners:

1) Right-angled Corner
2) Acute-angled turn

Also, the altitude of the quadrotor is affected during yaw around a corner. Therefore, the corner performances are analyzed with reference to the altitude of

5.2.2.1 Right-Angled Corner

During the rectangular mission profile (P_1) of the quadrotor, the quadrotor undergoes a right-angled turn at each of the waypoints. A quadrotor has to yaw about the vertical axis at waypoints in order to follow the mission path in Path P_1 making a right-angled coordinated turn.

Path characteristics

The following Figure 5.12 shows the altitude characteristics of the quadrotor in a quadrilateral mission path. The quadrotor exhibits altitude fluctuations throughout its path. It is also worth noting that, on each waypoint, the altitude of the quadrotor drops a certain height and then goes on to adjust the altitude. During this adjustment, the quadrotor overshoots the altitude, and then again, the controller tries to adjust the altitude by pitching down. This variation creates a wavy nature of the altitude along the

whole mission path. This plot illustrates the basic nature of the Pixhawk controller altitude controller. So, we can see that the quadrotor drops its altitude when reaching a waypoint and yawing in the direction of the next waypoint. This variation in altitude is further cleared with the scaled view of section A, as shown in Figure 5.13.

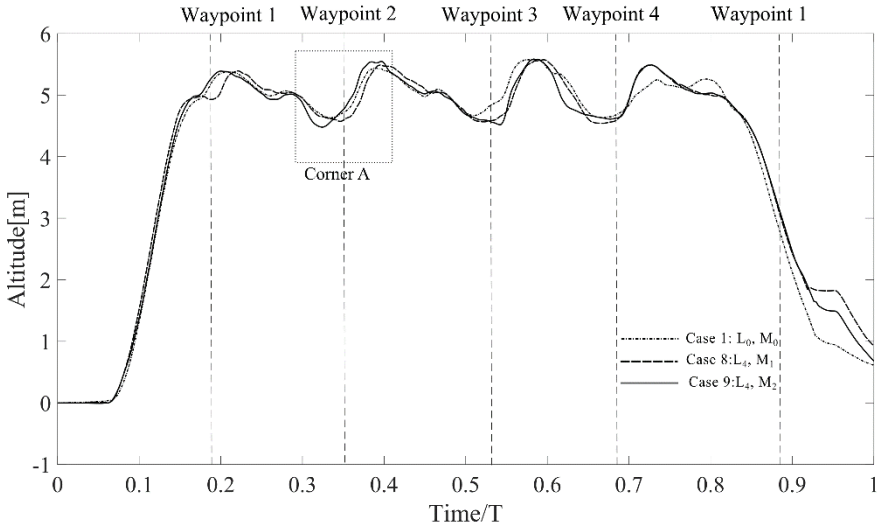

Figure 5.12: Variation of altitude over time for P_1 mission

In the figure above, the fluctuation of altitude at waypoint 2 of the quadrilateral mission profile is shown. We can see that, compared with the no-load condition, the additional tethered load increases the altitude overshoot and undershoot of the vehicle, in both the

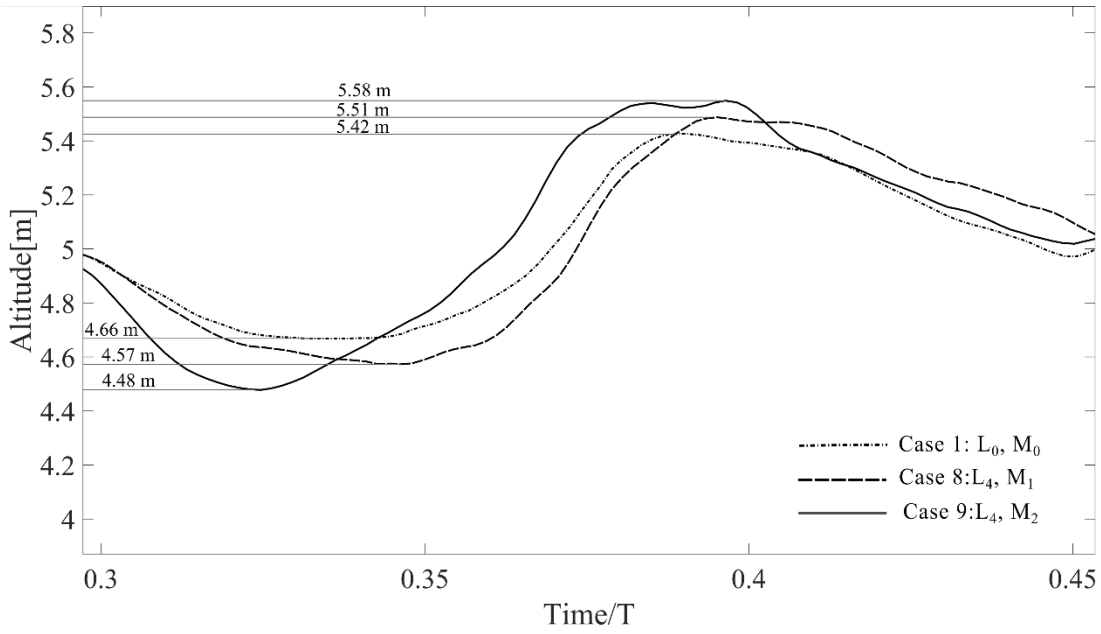

Figure 5.13: Variation of quadrotor altitude in path P_1 in Corner-A

upper and lower end of the set altitude. Considering the overall fluctuation of the quadrotor, compared to the no load condition, case 1, tethered payload condition, case

8, and case 9, fluctuates 23.68% and 44.73% more in both directions of set altitude respectively.

Again, compared to the no load condition, in case 1, the tethered payload with mass M_1, case 8, undershoots the set altitude of 5m by 2.47%; while in case 9, with tethered payload M_2, the quadrotor undershoots 52.94% over the set altitude at the waypoint. And similarly, when compared to the no load condition, in case 1, the tethered payload with mass M_1, case 8, overshoots the set altitude of 5m by 21.43%; while in case 9, with tethered payload M_2, the quadrotor overshoots 38.09% over the set altitude at the waypoint during a right-angled corner turn.

Moreover, with the increase in payload mass from M_1 to M_2, the altitude overshoot over the set altitude increases by 13.75%, while the altitude undershoots increase by 20.10%. Although the Pixhawk4 controller in itself tries to maintain the altitude of the vehicle, the additional load on the quadrotor is seen to increase the fluctuation in altitude, which may be because of the response of the controller to increased mass by providing extra thrust on the motor. This extra thrust on the motor causes the increased quadrotor momentum that causes the overshoot and undershoot in both of the scenarios.

5.2.2.2 Acute Angled Corner

During the Triangular mission profile (P_2) of the quadrotor, the quadrotor undergoes an acute-angled turn at each of the waypoints. A quadrotor has to yaw about the vertical axis at waypoints in order to follow the mission path in Path P_1 making a sharp coordinated turn. The inherent characteristics of the controller cause the quadrotor to move in a specific pattern, however, the addition of tethered payload will change the quadrotor's performance that of the no-load condition. The characteristics are analyzed in a similar fashion to that of the quadrilateral mission path profile, in order to have an insight into the effect of sharp turns on quadrotor attitude.

Path characteristics

The following Figure 5.14 shows the altitude characteristics of the quadrotor in a quadrilateral mission path. The quadrotor exhibits altitude fluctuations throughout its path. Although due to the same nature of the controller to handle the disturbances on a mission path, the overshoot and undershoot on a mission waypoint is still seen on the

triangular mission profile as well. The Following Figure 5.14 shows the variation in altitude during the different mission profiles.

In path P_2, the altitude of waypoint 2 is set at 10 m, while both 1 and 3 were set at 5 m.

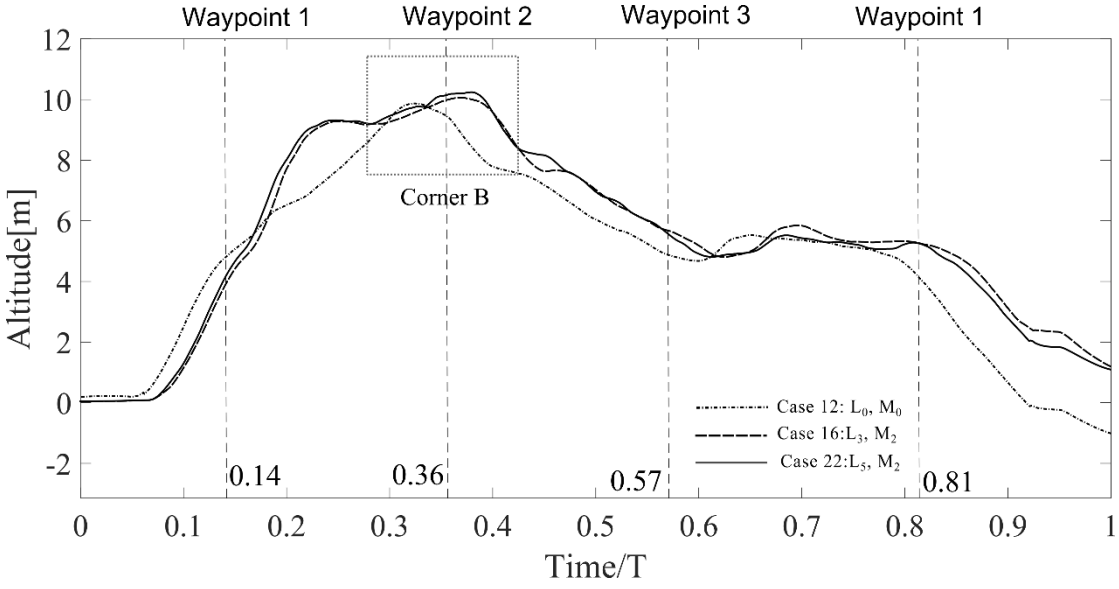

Figure 5.14: Variation of quadrotor altitude with time on path P_2

Although there seem to be disturbances all along the path of the vehicle, the wavy pattern on the waypoint is seen to have lower amplitude fluctuation all along the mission profile. To obtain more detailed information on altitude fluctuations with and without a load condition on the triangular mission, corner B is defined in Figure 5.14 to illustrate the altitude fluctuations more clearly.

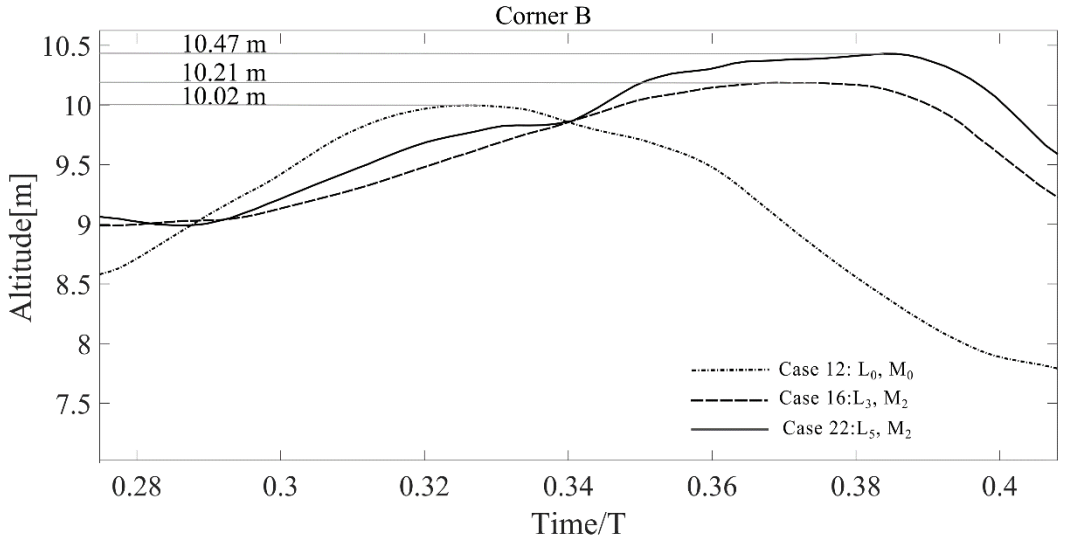

Figure 5.15: Variation of altitude on Corner-B with time

We can see from the above figure that, when the quadrotor ascends from waypoint 1 to waypoint 2 in path P_2, it overshoots the set altitude in all the cases. However, in comparison, the no-load condition is almost at the set altitude, and other cases with a payload mass on different tether lengths overshoot to a higher altitude. We can also notice that almost all the altitude curves become flat near the top of the altitude profile, this may have been due to the vehicle receiving the returning to altitude of 5m profile command as soon as it hits the top altitude, which prevents the quadrotor oscillation as it does not have to maintain the altitude on set value.

In Figure 5.15, we can see that, on no load condition on path P_2, case 12, the quadrotor overshoots just 0.2% of waypoint 2 set altitude, while case 16, M_2 payload suspended with L_3 tether of 0.5 m overshoots 2.1% more than the set altitude. But with cable length, $L_{3,}$ of 1m and the same payload mass, the overshoot over the set altitude by 4.7%. And when compared to the no-load condition, the 0.1 kg payload on a 1m suspension cable overshoots by 4.49%.

5.3 Landing

The landing segment of the autonomous mission path is where the payload returns to the launch site after completing the autonomous path by returning to waypoint 1 of the mission path. The landing segment of the mission involves an interplay of all the

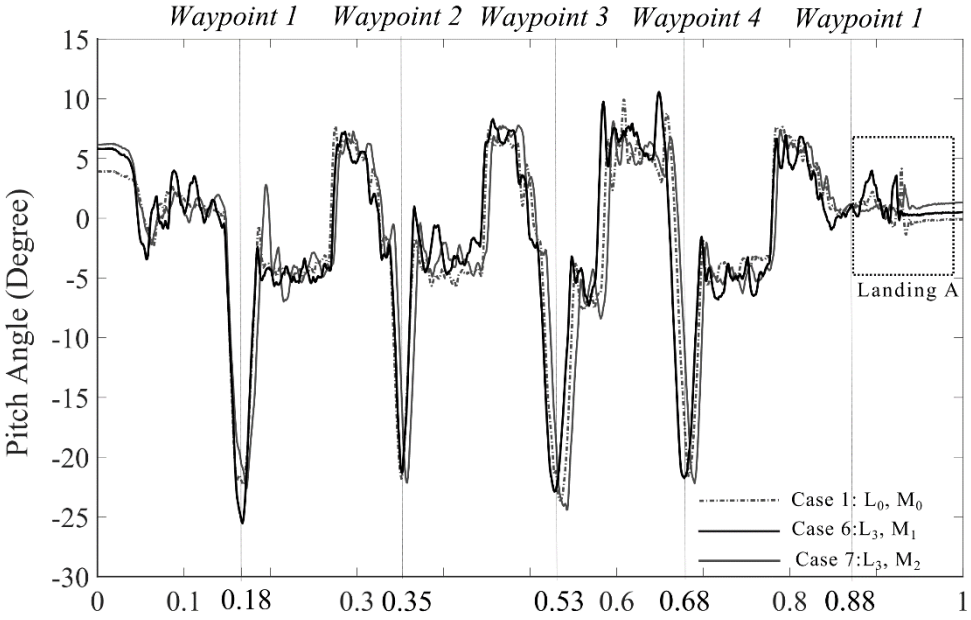

Figure 5.16: Pitch angle variation with Landing-A section

accumulated errors of the autonomous mission profile, and dynamics of slung payload while also maintaining the quadrotor stability under these conditions.

In Figure 5.16 above, the variation of pitch angle with time is plotted, highlighting the landing phase of the mission. Landing is a very short segment of an autonomous mission path; however, it is very critical for the safe delivery of payload and maintaining the integrity of the quadrotor. The landing segment A is shown in the figure below for details of the quadrotor pitch variation.

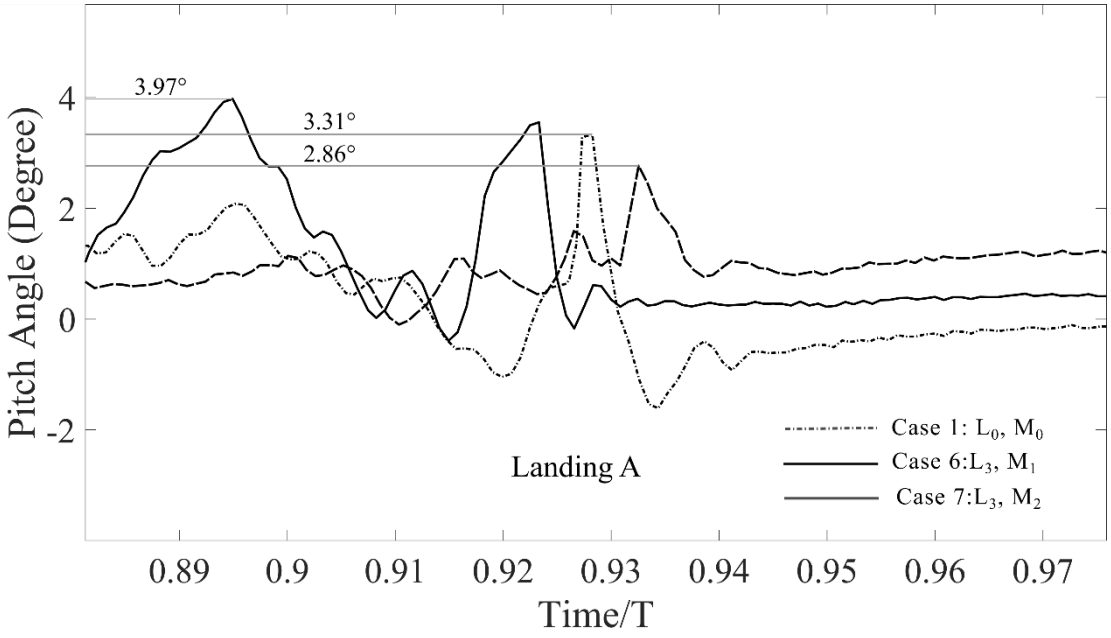

Figure 5.17: Variation of pitch on Landing-A section

In this figure, we can see the variation that occurs on quadrotor pitch, as the vehicle tries to land on the launch point. We can see that with maximum payload mass, case 7 experiences the most pitch fluctuations. From the figure, the no-load quadrotor experiences a maximum pitching angle of 3.31° during the landing of the quadrotor. But, interestingly, the case with 0.5 m (L_3) tether with a payload mass of M_1 has a spike of pitch angle during the end of the landing segment. Furthermore, the case with a maximum payload of M_2 and cable length L_3 requires a maximum pitching of 3.97° during the landing stage. This may have been because the vehicle adjusted to the payload disturbance as the payload lands by pitching up and down for a stable landing.

We can see that, with maximum tethered payload, the pitch angle of the quadrotor with tethered payload mass is 19.94% greater than in no load condition. But interestingly, the 0.1kg load condition shows a lower pitch angle amplitude than in the no-load

condition by 13.59%. This abnormality may have occurred due to the accumulation of errors in the whole autonomous path.

CHAPTER SIX: CONCLUSIONS AND RECOMMENDATIONS

6.1 Conclusions

The study investigated the effect of tether-suspended payload mass (M_p) on quadrotor attitude and path, by conducting an autonomous flight mission with quadrotor. For the sake of analysis, the total mission path segments were broken down into three segments, take-off, cruise/trajectory flight, and landing. Through experimentation and numerical analysis in MATLAB, the study successfully characterized the behavior of the quadrotor equipped with a Pixhawk 4 controller. The analysis of pitch and roll characteristics has revealed significant fluctuations in these attitude parameters, particularly during the critical phases of takeoff and cruising.

During takeoff, it is evident that the quadrotor engages in dynamic adjustments to compensate for the added instability caused by the suspended payload. The pitch angle experiences notable fluctuations, with a 108% increase on no-load quadrotor pitch angle correction with 0.2 kg payload mass and a 47.28% increase with 0.1kg of payload mass. Also, an increase in payload mass from 0.1kg to 0.2 kg increased the pitch angle oscillation amplitude by 41.69%. Similarly, the roll angle amplitude also seems to experience a 22.8% increased oscillation amplitude with increasing weight, and a 20.14% increase in roll angle amplitude when cable length was doubled from 0.5m with the same payload.

Furthermore, the trajectory flight performance, specifically the straight-line cruise, reveals further insights. The quadrotor's pitch angle during this phase exhibits a pattern of adjustments aimed at maintaining altitude, thus, creating two distinct regions of pitch fluctuations. On the first region, between two payloads, an increase in payload mass for the same length of tether results in 27.10% more amplitude of pitch oscillation. And on the second region, the pitching angle for 0.2 kg mass was found to be 14.24% more than that of the no-load condition. Further, in comparison with 0.1 kg payload, 0.2 kg payload exhibits an 8.64% increase in amplitude of pitch oscillation. Also, the increase in speed of the quadrotor was found to decrease the time period of pitch oscillation by 28.3%. In addition to the pitch oscillation, the quadrotor was found to exhibit a roll angle oscillation along the entire flight path. Upon further analysis, roll angle oscillation amplitude increases by 3.41% from no load condition compared to 0.1 kg payload; and

a 10.93% increase in roll angle amplitude when the payload is increased from 0.1 kg to 0.2 kg.

In addition to a straight-line cruise, when the quadrotor turns on each waypoint, it overshoots and undershoots its set altitude showing the altitude oscillation in both the quadrilateral mission path and triangular mission path. When analyzing the altitude profile of the quadrilateral mission path, compared to the no load condition, tethered payload condition, with 0.1 kg and 0.2 kg payload, fluctuate 23.68% and 44.73% more in both directions of set altitude respectively. Similarly, on the triangular mission P_2, the quadrotor has to take a sharp acute turn compared with the path P_1. During this mission, P_2, the payload with the longest cable length overshoots the most, 4.7%, above the altitude setpoint. And when compared to the no-load condition, the 0.1 kg payload on a 1m suspension cable overshoots by 4.49%.

Lastly, During the landing phase of the flight, the quadrotor pitch angle amplitude increases by 19.94% when a 0.2 kg payload is attached to the quadrotor with 0.5m tether length than in no load condition. But interestingly, the 0.1kg load condition shows a lower pitch angle amplitude than in the no-load condition by 13.59%. This abnormality may have occurred due to the accumulation of errors in the whole autonomous path. So definite relationship during landing should be further studied.

These findings emphasize the need for careful consideration of payload effects in autonomous quadrotor missions. The observed fluctuations in pitch and roll angles highlight the challenges posed by varying payload conditions. Such insights are crucial for designing effective control strategies and optimizing autonomous flight performance. As drone technology continues to evolve and find applications in diverse fields, this research contributes to the understanding of quadrotor behavior under different payload conditions, paving the way for safer and more efficient autonomous missions.

6.2 Recommendations

Based on the study's outcomes, several key recommendations can be made for future research and the development of quadrotor systems:

1) Payload Damping System: Designing and implementing a payload damping system can help mitigate the oscillations induced by increased payload mass.

Such a system could enhance the stability and responsiveness of the quadrotor, especially when carrying heavier loads.

2) Landing Segment of the Flight: Due to the complexity and limitation of resources, the landing segment of the flight could find better refinement on data and details in this study. So, studying the landing segment of the plot would be very useful to develop the means of safe payload landing, and return of vehicle to the launch site in real-world situations.
3) Propeller and Motor Selection: Further investigation can be made with a set of BLDC motors having higher thrust power and corresponding propeller. This could help to analyze the effect of payload with a number of different masses; as lower thrust per motor has limited this study to only 2 payload mass variations have limited this study. With increased payload capacity a range of
4) Advanced Control Strategies: Developing advanced control strategies, such as adaptive control or fuzzy control, may enhance the quadrotor's response time and performance when dealing with destabilizing factors, such as varying payload mass and cable lengths.
5) Path Planning Algorithms: Integrating sophisticated path planning algorithms can aid in optimizing the quadrotor's trajectory, considering the vehicle's speed and payload characteristics. This could reduce unnecessary delays and improve mission efficiency.
6) Comparative Studies: Conducting comparative studies with other quadrotor controllers and platforms could offer valuable insights into the strengths and weaknesses of the Pixhawk 4 controller and help identify potential areas for improvement.
7) Payload-Specific Control Tuning: Depending on the specific payload type, it may be beneficial to develop customized control tuning strategies to optimize the quadrotor's performance when carrying different types of loads, such as cameras, sensors, or packages.

By addressing these recommendations, future research can further enhance the understanding and control of quadrotor systems when dealing with tether-suspended payload mass, thereby enhancing the means of quadrotor payload delivery.

REFERENCES

Alkomy, H., & Shan, J. (2021). Vibration reduction of a quadrotor with a cable-suspended payload using polynomial trajectories. *Nonlinear Dynamics*, *104*(4), 3713–3735. https://doi.org/10.1007/S11071-021-06464-6/FIGURES/23

Alothman, Y., Jasim, W., & Gu, D. (2015). Quad-rotor lifting-transporting cable-suspended payloads control. *2015 21st International Conference on Automation and Computing: Automation, Computing and Manufacturing for New Economic Growth, ICAC 2015*. https://doi.org/10.1109/ICONAC.2015.7313996

Bhattarai, S., Poudel, K. R., Bhatta, N., Mahat, S., Bhattrai, S., & Thapa Magar, K. S. (2018). Modeling and development of baseline guidance navigation and control system for medical delivery UAV. *AIAA Information Systems-AIAA Infotech at Aerospace, 2018*. https://doi.org/10.2514/6.2018-0508

Brescianini, D. ;, Hehn, M., ; D'andrea, R., Brescianini, D., & D'andrea, R. (2013). *ETH Library Nonlinear Quadrocopter Attitude Control Technical Report Nonlinear Quadrocopter Attitude Control Technical Report*. https://doi.org/10.3929/ethz-a-009970340

Emran, B. J., & Najjaran, H. (2018). A review of quadrotor: An underactuated mechanical system. *Annual Reviews in Control*, *46*, 165–180. https://doi.org/10.1016/J.ARCONTROL.2018.10.009

Estevez, J., Lopez-Guede, J. M., Garate, G., & Graña, M. (2021). A Hybrid Control Approach for the Swing Free Transportation of a Double Pendulum with a Quadrotor. *Applied Sciences 2021, Vol. 11, Page 5487*, *11*(12), 5487. https://doi.org/10.3390/APP11125487

Faust, A., Palunko, I., Cruz, P., Fierro, R., & Tapia, L. (2017). Automated aerial suspended cargo delivery through reinforcement learning. *Artificial Intelligence*, *247*, 381–398. https://doi.org/10.1016/J.ARTINT.2014.11.009

Goodarzi, F. A. (2016). Autonomous aerial payload delivery with quadrotor using varying length cable. *International Conference on Advanced Mechatronic Systems, ICAMechS*, *0*, 394–399. https://doi.org/10.1109/ICAMECHS.2016.7813481

Guerrero-Sánchez, M. E., Mercado-Ravell, D. A., Lozano, R., & García-Beltrán, C. D. (2017). Swing-attenuation for a quadrotor transporting a cable-suspended payload. *ISA Transactions*, *68*. https://doi.org/10.1016/j.isatra.2017.01.027

Guo, J., Li, L., Li, K., & Wang, R. (2013). An adaptive fuzzy-sliding lateral control strategy of automated vehicles based on vision navigation. *Vehicle System Dynamics*, *51*(10), 1502–1517. https://doi.org/10.1080/00423114.2013.811789

Han, B., Zhou, Y., Deveerasetty, K. K., & Hu, C. (2018). A review of control algorithms for quadrotor. *2018 IEEE International Conference on Information and Automation, ICIA 2018*, 951–956. https://doi.org/10.1109/ICINFA.2018.8812437

Kevin, S., & Graham, I. (2019). *Development of a Quadrotor Slung Payload System*.

Lee, J.-W., Xuan-Mung, N., Phi Nguyen, N., & Kyung Hong, S. (2019). Adaptive altitude flight control of quadcopter under ground effect and time-varying load: theory and experiments. *Journal of Vibration and Control*, *0*(0), 1–11. https://doi.org/10.1177/10775463211050169

Meissen, C., Klausen, K., Arcak, M., Fossen, T. I., & Packard, A. (2017). Passivity-based Formation Control for UAVs with a Suspended Load. *IFAC-PapersOnLine*, *50*(1), 13150–13155. https://doi.org/10.1016/J.IFACOL.2017.08.2169

Nicotra, M. M., Garone, E., Naldi, R., & Marconi, L. (2014). Nested saturation control of an UAV carrying a suspended load. *Proceedings of the American Control Conference*, 3585–3590. https://doi.org/10.1109/ACC.2014.6859222

Omar, H. M., Akram, R., Mukras, S. M. S., & Mahvouz, A. A. (2022). Recent advances and challenges in controlling quadrotors with suspended loads. In *Alexandria Engineering Journal*. Elsevier B.V. https://doi.org/10.1016/j.aej.2022.08.001

Omar, H. M., Fortuna, L., Choi, Y., & Omar, H. M. (2022). Hardware-In-the-Loop Simulation of Time-Delayed Anti-Swing Controller for Quadrotor with Suspended Load. *Applied Sciences 2022, Vol. 12, Page 1706*, *12*(3), 1706. https://doi.org/10.3390/APP12031706

Palunko, I., Fierro, R., & Cruz, P. (2012). Trajectory generation for swing-free maneuvers of a quadrotor with suspended payload: A dynamic programming

approach. *Proceedings - IEEE International Conference on Robotics and Automation*, 2691–2697. https://doi.org/10.1109/ICRA.2012.6225213

Pounds, P. E. I., Bersak, D. R., & Dollar, A. M. (2012). Stability of small-scale UAV helicopters and quadrotors with added payload mass under PID control. *Autonomous Robots 2012 33:1*, *33*(1), 129–142. https://doi.org/10.1007/S10514-012-9280-5

PX4 User Guide. (n.d.). Retrieved June 13, 2023, from https://docs.px4.io/main/en/

Qian, L., Graham, S., & Liu, H. H. T. (n.d.). *IEEE/ASME TRANSACTIONS ON MECHATRONICS (TMECH) i Guidance and Control Law Design for a Slung Payload in Autonomous Landing A Drone Delivery Case Study*.

Qian, L., & Liu, H. H. T. (2017). Dynamics and control of a quadrotor with a cable suspended payload. *Canadian Conference on Electrical and Computer Engineering*. https://doi.org/10.1109/CCECE.2017.7946750

Roy, R., Islam, M., Sadman, N., Mahmud, M. A. P., Gupta, K. D., & Ahsan, M. M. (2021). A Review on Comparative Remarks, Performance Evaluation and Improvement Strategies of Quadrotor Controllers. *Technologies 2021, Vol. 9, Page 37*, *9*(2), 37. https://doi.org/10.3390/TECHNOLOGIES9020037

Sunghun, J., & su, kim hyun. (2017). Analysis of Amazon Prime Air UAV Delivery Service. *Journal of Knowledge Information Technology and Systems*, *12*(2), 253–266. https://doi.org/10.34163/JKITS.2017.12.2.005

Us, K. Y., Cevher, A., Sever, M., & Kirli, A. (2019). On the Effect of Slung Load on Quadrotor Performance. *Procedia Computer Science*, *158*, 346–354. https://doi.org/10.1016/J.PROCS.2019.09.061

Xian, B., Wang, S., & Yang, S. (2020). An Online Trajectory Planning Approach for a Quadrotor UAV with a Slung Payload. *IEEE Transactions on Industrial Electronics*, *67*(8), 6669–6678. https://doi.org/10.1109/TIE.2019.2938493

Yi, K., Gu, F., Yang, L., He, Y., & Han, J. (2017). Sliding mode control for a quadrotor slung load system. *Chinese Control Conference, CCC*, 3697–3703. https://doi.org/10.23919/CHICC.2017.8027934

Zhou, X., Liu, R., Zhang, J., & Zhang, X. (2016). Stabilization of a quadrotor with uncertain suspended load using sliding mode control. *Proceedings of the ASME Design Engineering Technical Conference, 5A-2016*. https://doi.org/10.1115/DETC2016-60060

APPENDIX A: DRONE ASSEMBLY PARTS AND MODULES

1. Frame: S500 Generic- X Configuration

Figure A.1: S500 Frame X config

2. Propellers: 1045

Figure A.2: 1045 Propeller

3. Electronic Speed Controller (ESC): 30 A

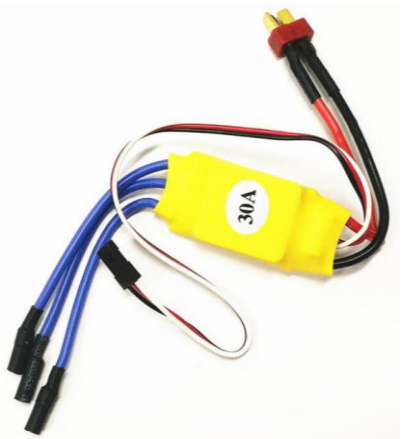

Figure A.3: Electronic Speed Controller 30A

4. Brushless DC Motors (BLDC): 980 KV (Qty:- 4)

Figure A.4: BLDC motors 980 KV

5. Battery: 3700 MAH Battery

Figure A.5: Li-Po Battery 40C (3700 MAH)

6. M8N GPS Module

Figure A.6: M8N GPS Module

7. Power Modul: PM07

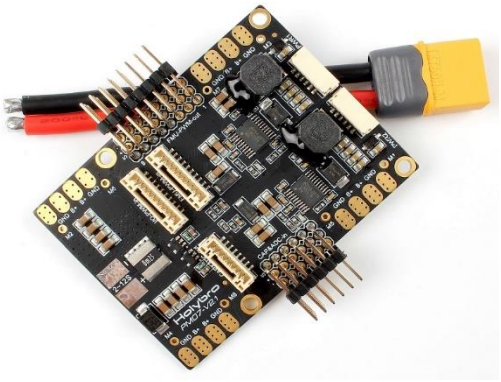

Figure A.7: Power Module (PM07)

8. Pixhawk4® Controller:

Figure A.8: Pixhawk 4® Controller

9. Suspended Load

Figure A.9: Load for Suspension

10. Telemetry:

Figure A.10: Telemetry Set Transmitter and Reciever

11. PPM RC Reciever: Flysky FS-IA6B

Figure A.11: PPM RC Reciever

APPENDIX B: DRONE ASSEMBLY SCHEMATIC

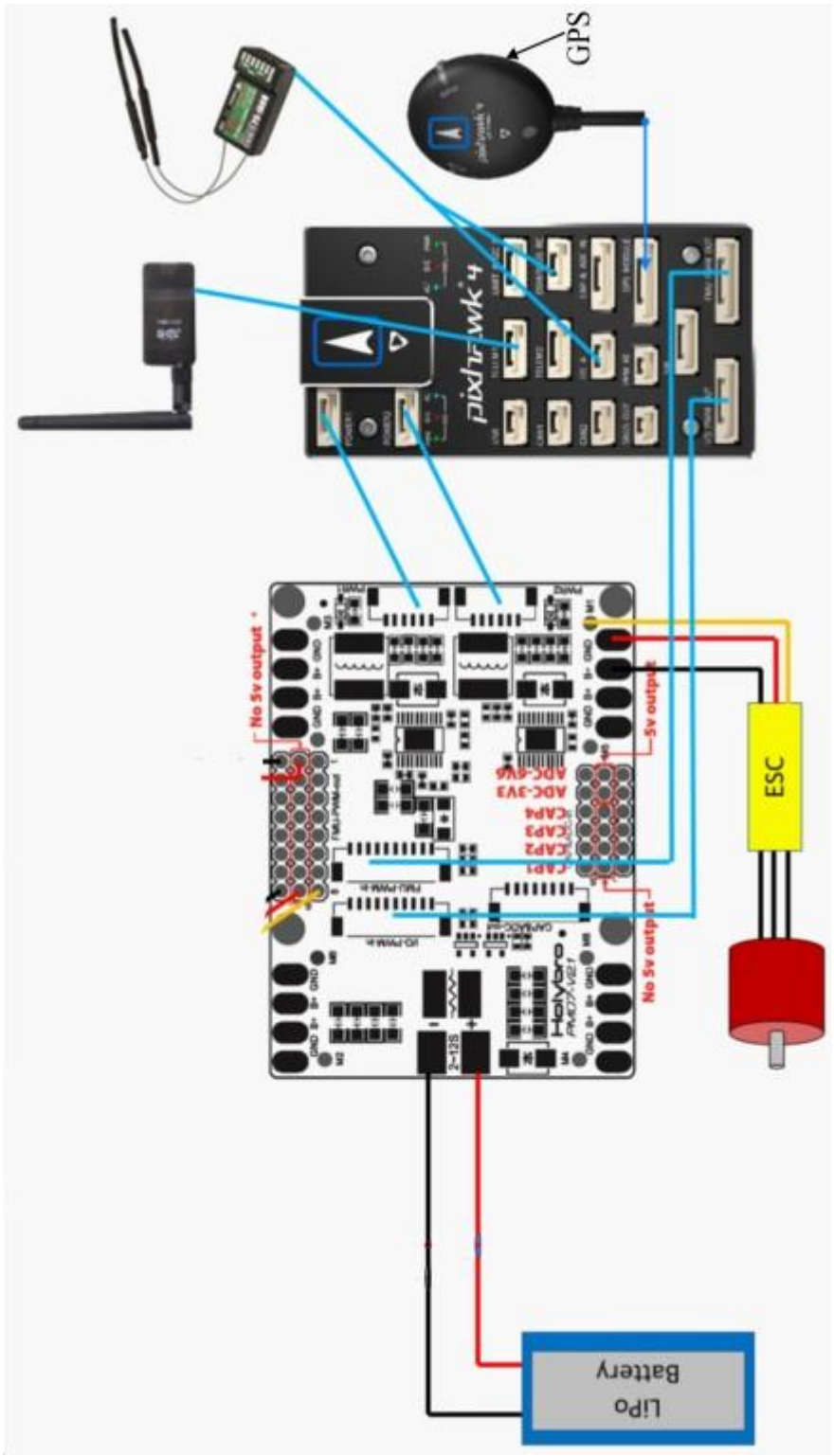

Figure A.12: Schematic Diagram for assembly of the Quadrotor with Pixhawk Controller

APPENDIX C: MATLAB PROGRAMS

1. MATLAB program for post processing the Pixhawk Flight data

```
% Postprocess the slung mass on quadcopter
clear;clc; %close all;
dataDir = 'slung_mass_data';
% Mission= 2;
Mission  = input('enter mission number: ');
% tether length in cm
L       = input('enter tether length in cm: ');
%slung mass in g
m       = input('enter slung mass in gram: ');
% string
strings = ["sensor_combined_0" "vehicle_local_position_0"
"vehicle_attitude_0"];
% sindex= 1;
sindex  = input('string index ');
string= char(strings(sindex));
% read data
data=tdfread([dataDir '\M' num2str(Mission) '_' num2str(m) 'g_'
num2str(L) ...
    strcat('cm_',string) '.csv']);
data=struct2array(data);%Converting data format for computation
%Calculating time from raw data
time = (data(:,1)-data(1,1))/1e6;
T=time(end);
% disp([T]);

%% Plot Vibration Data
if sindex==1
    accelX = data(:, 7);
    accelY = data(:, 8);
    accelZ = data(:, 9);
    % vibration = sqrt((accelX.^2 + accelY.^2 + accelZ.^2)/3);
    accelSquaredSum = accelX.^2 + accelY.^2 + accelZ.^2;
    vibration=sqrt(accelSquaredSum/3);
    F = length(data)/time(end); %Sampling Rate
    %cropping data for time selection
    start_time= input('enter start time for analysis:');
    end_time= input('enter end time for analysis: ');
    crop = [int16(start_time*F) int16(end_time*F)];
    %Plotting Vibration over Time
    figure(1)
    hold on;

plot(time(crop(1):crop(2)),vibration(crop(1):crop(2)),'LineWidth',1);
    xlabel('Time [s]');
    ylabel('Vibrating Acceleration(m/s^2)');
    hold on;
%     title('Vibration Over Time');
    %Compute sampling rate
    F = length(data)/time(end);
    crop = [int16(9*F) int16(50*F)];
    % perform frequency analysis
    simple_fft(vibration(crop(1):crop(2)),F);
end
%% Plot path data
```

```
%Vertical Path plot for the altitude
if sindex == 2
    figure(4)
    hold on;
    plot(time/T,(data(1,8)-data(:,8))/5,'LineWidth',2);
    xlabel('Time/T');
    ylabel('Altitude[m]');
%     title(['Alitude plot for the Mission', num2str(Mission),'p_'],
num2str(Mission));
%     print('-dpdf',['plots/vpath_M' num2str(Mission) '_' num2str(m)
'g_' num2str(L) 'cm_zt.pdf']);
%Visualise path
    figure(5)
    hold on;
%     plotting top view path of the quadrotor
    plot(data(:,6),data(:,7),'LineWidth',2); xlabel('X [m]');
ylabel('Y [m]');
%     print('-dpdf',['plots/path_M' num2str(Mission) '_' num2str(m)
'g_' num2str(L) 'cm_xy.pdf']);
end
if sindex==3
    n=length(data)% n is no. of a data rows in file
    angles=zeros(n,3); % empty angle (psi theta phi) matrix to append
    for i=1:n
        q=[data(i,3),data(i,4),data(i,5),data(i,6)] % quaternion
assembled
        [angles(i,1),angles(i,2),angles(i,3)]=(quat2angle(q)) %
returns euler angle in radian
    end
    angles=rad2deg(angles); % converting the euler angle from radian
to degree
    time = (data(:,1)-data(1,1))/1e6;
    figure(1); %% yaw angle (psi) plot
    plot(time/time(end),angles(:,1),'Linewidth',2); xlabel('Time/T');
ylabel('Yaw Angle');
    hold on;
    figure(2); %% pitch angle (theta) plot
    plot(time/time(end),angles(:,2),'Linewidth',2); xlabel('Time/T');
ylabel('Pitch Angle');
    hold on;
    figure(3); %% roll angle ( phi) plot
    plot(time/time(end),angles(:,3),'Linewidth',2); xlabel('Time/T');
ylabel('Roll Angle');
    hold on;
end
```

2. MATLAB Function for fast fourier Transform

```
function [] = simple_fft(data,Fs)
L=length(data);
% Simple FFT function
Y = fft(data,L);

% amplitude amplitude
f = Fs*(0:(L/2))/L;
P2 = abs(Y/L);
P1 = P2(1:L/2+1);
P1(2:end-1) = 2*P1(2:end-1);
% plot amplitude spectrum
figure(2)
hold on;
plot(f(2:end),P1(2:end),'LineWidth',1)
% print('-dpdf',['plots/FFT_M' num2str(Mission) '_'
num2str(m) 'g_' num2str(L) 'cm_vibrations.pdf'])
xlabel('Frequency (Hz)')
ylabel('Amplitude')
set(figure(1), 'units', 'centimeters','position', [ 20 5
15 10])
set(gca,'fontsize',10,'FontName','times')
%%
% power spectrum
Pyy = Y.*conj(Y)/L;   % PSD
f = Fs/L*(0:L/2-1);
% plot power spectrum
figure(3)
hold on;
plot(f(2:end),Pyy(2:end/2),'LineWidth',1)
xlabel('Frequency (Hz)')
ylabel('PSD')
set(figure(3), 'units', 'centimeters','position', [ 20 5
15 10])
set(gca,'fontsize',10,'FontName','times')
end
```